



POLITECNICO
MILANO 1863

RE.PUBLIC@POLIMI

Research Publications at Politecnico di Milano

Post-Print

This is the accepted version of:

J.D. Biggs, G. Livornese

Control of a Thrust-Vectoring CubeSat Using a Single Variable-Speed Control Moment Gyroscope

Journal of Guidance Control and Dynamics, Vol. 43, N. 10, 2020, p. 1865-1880

doi:10.2514/1.G005181

The final publication is available at <https://doi.org/10.2514/1.G005181>

Access to the published version may require subscription.

When citing this work, cite the original published paper.

Permanent link to this version

<http://hdl.handle.net/11311/1145520>

Control of a thrust-vectoring CubeSat Using a Single Variable Speed Control Moment Gyro

James D. Biggs * and Gaetano Livornese †

Polytechnic of Milan

A minimal actuator design is proposed for orbit-attitude control of a spacecraft. The actuator design includes a single thruster, fixed in the body frame, and a Variable Speed Control Moment Gyro (VSCMG) used for thrust-vectoring. It is known that the full-attitude cannot be controlled using a single VSCMG, but that a single axis is controllable. This paper develops a nonlinear control that is able to vector the thruster at discrete intervals or continuously. The closed-loop stability of the system is proved using Lyapunov stability theory for each control law. These control laws could enable high-maneuuvrability of CubeSats, utilizing either a single chemical (impulsive) or electric thruster (continuous). The controls are demonstrated, in simulation, with an application to a 12U CubeSat rendezvous utilizing a single throttling electric thruster.

*Associate Professor, Department of Aerospace Science and Technology, jamesdouglas.biggs@polimi.it

†Graduate student, Department of Aerospace Science and Technology, gaetano.livornese@mail.polimi.it

I. Introduction

Space technology is developing at an accelerating rate; propulsion technology is being used to extend mission life and enable new applications and miniaturized spacecraft, such as CubeSats, are opening space to a wider community, massively increasing commercialization opportunities. The possibility of CubeSats being used in a range of applications can now be realized due to the extensive range of commercial off the shelf actuators and sensors available. However, there are still opportunities for considerable mass savings by exploiting new designs, new actuator technology and employing new types of control algorithms. In this paper, a conceptual Cubesat is proposed [1] which employs one thruster for orbit maneuvering and a Variable Speed Control Moment Gyro (VSCMG) for thrust-vectoring [2]. This actuator configuration can allow high-maneuverability in-orbit using a minimal number of actuators. Using only two actuators can help to minimize the mass and volume requirement for the attitude and orbit control system. In addition, if used with other actuators for three-axis control and these actuators fail, then control of the thrust direction can be maintained.

It is well known that a single VSCMG cannot control the full-attitude of a spacecraft. However, this conceptual CubeSat only requires the pointing of the thruster which is controllable using a single VSCMG. This enables controls to be developed considering the reduced-attitude control problem [3]. The reduced-attitude control problem has been utilized to relax the control requirements of staring mode spacecraft [4]. However, in such systems the actuators employed have considered using multiple reaction wheels (RW) and thrusters to perform the maneuvers. In contrast this paper addresses the problem of spacecraft attitude control with a single VSCMG [5], which can be viewed as a hybrid of a RW and a control moment gyro (CMG) [6]. CMGs are known to be more power efficient than RWs while they suffer singularity problems in their control laws; while RWs are not capable of high torque performance and require frequent de-saturation[7–9]. Over the next decade, it is likely that there will be a higher demand for new momentum exchange devices able to overcome the shortfalls in current technology which will be competitive in terms of performances and power efficiency [10].

Most of the strategies for spacecraft attitude control have been developed for fully actuated systems, where the actuators can simultaneously control each degree of freedom of the spacecraft. However, under-actuated controls have been developed for full-attitude control including the use of two reactions wheels (with the assumption of zero total angular momentum) [11, 12], two continuous inputs (with the assumption of axis symmetry) [13, 14], four impulsive thrusters [15] and two CMGs [16–18]. However, by considering the reduced-attitude control problem, the minimal number of actuators could be further decreased while maintaining controllability. In H. Yoon and P. Tsotras [20] the control of a spacecraft with a single VSCMG is considered. In [20] a single VSCMG is used for angular velocity stabilisation and line-of-sight control. Moreover, a nonlinear controller is developed for de-tumbling, while a mixed multistage nonlinear/linear controller is developed to achieve the line-of-sight pointing. The development of a control that could enable line-of-sight tracking was not considered. In addition, [20] uses Euler angles (local-coordinates) to

develop the control laws which are less-suited to control design of highly-maneuverable spacecraft performing large re-orientations than globally defined co-ordinates.

In this paper a co-ordinate free, nonlinear control law is developed for rest-to-rest thrust-vectoring and tracking modes. An analysis of the control laws is undertaken to determine the closed-loop stability of the system. Finally, The control algorithms developed are applied to a rendezvous problem where the chaser spacecraft is a 12 U CubeSat with a single electric (continuous) thruster and a VSCMG used for thrust-vector tracking. A robustness analysis which includes the thruster misalignment with the principal axis is also undertaken in simulation.

II. Problem formulation

The proposed control problem consists of a coupled process of orbit and attitude control. Firstly, a feedback control for the orbital maneuver is implemented generating an ideal force profile. This feedback control is tuned so that the required thrust magnitude is feasible. The magnitude of the ideal force is then matched as closely as possible by the thruster; while the direction of the ideal force is tracked using a VSCMG. The problem formulation is detailed in the following subsections.

A. Generating the desired thrust-vectorized direction

In this paper, a spacecraft rendezvous problem is considered using the Hill's reference frame [21]. The relative motion between two spacecrafts, with one satellite that is controlled (the chaser) is required to maneuver onto a target. To describe the relative motion equations, a Cartesian Local-Vertical, Local-Horizontal (LVLH) frame is introduced. This frame is attached to the chief satellite, as shown in Fig.1.

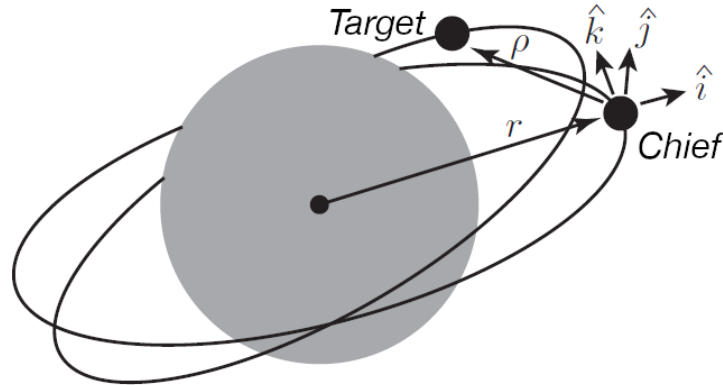


Fig. 1 Relative motion scheme.

In this coordinate frame, \hat{i} lies in the chief's radial direction, \hat{k} lies in the direction of the chief's orbital angular momentum, and \hat{j} completes the right-handed orthonormal triad. \hat{i} and \hat{j} directions correspond to the in-plane motion, and \hat{k} corresponds to the out-of-plane motion. This coordinate frame will be referred to as the orbit frame $O = \{\hat{i} \ \hat{j} \ \hat{k}\}$

and rotates with respect to an inertially fixed frame $N = \{\hat{n}_1 \ \hat{n}_2 \ \hat{n}_3\}$. In general, the equations of motion can be expressed in the form:

$$\rho'' = f(\rho', \rho) + a \quad (1)$$

where ρ'' and ρ' denote the time derivatives with respect to the LVLH O frame, $a = [a_x \ a_y \ a_z]^T$ is the acceleration vector, and

$$\rho = x\hat{i} + y\hat{j} + z\hat{k} \quad (2)$$

Within the control synthesis it is necessary to compute a dynamic ideal force continuously over the duration of the maneuver. We assume that a feedback law is implemented to control the orbit of the form:

$$a = f_2(\rho, \rho') \quad (3)$$

The design of such a controller has been extensively studied, for example in [21], and so is not detailed here. From (3) it is possible to continuously compute the desired thrust magnitude T defined by

$$T = m_{S/C} ||a|| \quad (4)$$

where $m_{S/C}$ is the mass of the spacecraft. The only constraint imposed on the control design is available force magnitude of the thruster. The desired thrust-vector direction Γ_d^N , where N denotes the vector evaluated in the basis of the inertial frame is then

$$\Gamma_d^N = A_{O/N}^T \Gamma_d^O \quad (5)$$

with

$$\Gamma_d^O = \frac{a}{||a||} \quad (6)$$

where the superscript O denotes that the vector is defined in the basis of the orbit frame and where $A_{O/N}$ is a rotation matrix describing the relative orientation of the orbit frame with respect to the inertial frame. Therefore, the desired pointing direction for the spacecraft is given by Γ_d^N . In this paper we consider using an electric thruster such that Γ_d^N must be tracked continuously. If using a single chemical (impulsive) thruster, then at each impulse n a required Delta V should be computed. In this case the attitude control requires n rest-to-rest maneuvers to be performed before each thruster firing [1].

B. Spacecraft and VSCMG dynamics

The attitude dynamics of the spacecraft utilizing a single thruster and a VSCMG are described here. We define a body fixed frame $B = \{\hat{b}_1, \hat{b}_2, \hat{b}_3\}$ and a gimbal frame $G = \{\hat{s}, \hat{t}, \hat{g}\}$ where the gimbal frame is attached to the VSCMG as shown in Fig.2.

The body frame and the gimbal frame are related by the following rotation:

$$\begin{bmatrix} \hat{s} \\ \hat{t} \\ \hat{g} \end{bmatrix} = \begin{bmatrix} \cos \gamma & \sin \gamma & 0 \\ -\sin \gamma & \cos \gamma & 0 \\ 0 & 0 & 1 \end{bmatrix} \begin{bmatrix} \hat{b}_1 \\ \hat{b}_2 \\ \hat{b}_3 \end{bmatrix} \quad (7)$$

where γ is the gimbal angle and where the total angular momentum \mathbf{h} of the system can be expressed as

$$\mathbf{h} = J\boldsymbol{\omega} + I_{cg}\dot{\gamma}\hat{g} + I_{ws}\Omega\hat{s} \quad (8)$$

Where J is the inertia matrix of the spacecraft including the VSCMG, Ω is the VSCMG wheel angular velocity with respect to the spacecraft, I_{cg} is the total inertia along the gimbal axis \hat{g} and I_{ws} is the total inertia along the wheel axis \hat{s} , while the VSCMG total inertia along \hat{t} is assumed negligible. It is assumed here that J is constant. Moreover, we assume that the inertia of the VSCMG which is time-varying in the body frame is negligible compared to the inertia of the spacecraft. The additional terms included in the dynamics if considering a time-varying J can be found in [19].

It follows from the transport theorem [19] that the inertial derivative of Eq. (8) is:

$${}^N\frac{d}{dt}(\mathbf{h}) = {}^B\frac{d}{dt}(J\boldsymbol{\omega} + I_{cg}\dot{\gamma}\hat{g} + I_{ws}\Omega\hat{s}) + \boldsymbol{\omega} \times (J\boldsymbol{\omega} + I_{cg}\dot{\gamma}\hat{g} + I_{ws}\Omega\hat{s}) \quad (9)$$

where

$${}^B\frac{d}{dt}(J\boldsymbol{\omega} + I_{cg}\dot{\gamma}\hat{g} + I_{ws}\Omega\hat{s}) = J\dot{\boldsymbol{\omega}} + J\boldsymbol{\omega} + I_{cg}\ddot{\gamma}\hat{g} + I_{ws}\dot{\Omega}\hat{s} + I_{ws}\Omega\dot{\gamma}\hat{t} \quad (10)$$

where the left superscript on the derivative operator indicates in which frame the derivative is taken with respect to. For simplicity of notation and going forward, $\dot{\mathbf{x}} = {}^B\frac{dx}{dt}$ denotes a derivative of an arbitrary vector \mathbf{x} taken with respect to the body frame. Eq. (10) can be simplified considering the conservation of angular momentum since ${}^N d/dt(\mathbf{h}) = 0$ and, with the assumption that the inertia matrix J is constant, $\dot{J} = 0$. Again, the total spacecraft inertia J is not constant in practise because the VSCMG is rotating around the gimbal axis \hat{g} . This contribution will be considered in future works when considering disturbances and robust control. Finally, the effect of the term $\ddot{\gamma}$ is assumed to be negligible as justified in [20], thus

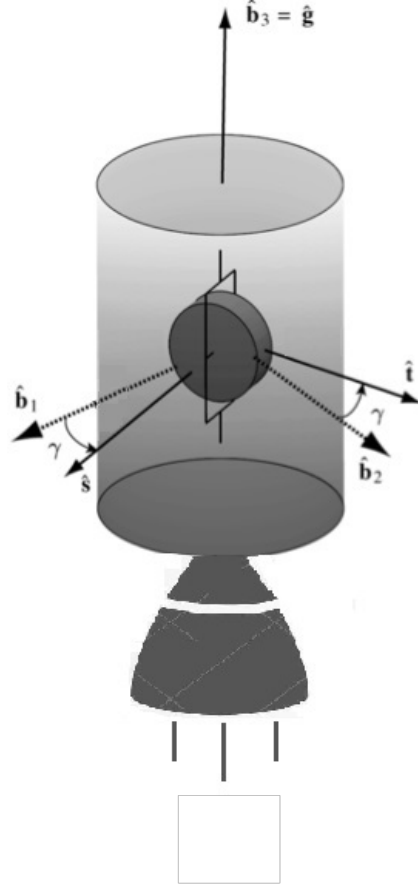


Fig. 2 System configuration.

$$J\dot{\omega} = J\omega \times \omega - I_{cg}\dot{\gamma}\omega \times \hat{g} - I_{ws}\Omega\omega \times \hat{s} - I_{ws}\dot{\Omega}\hat{s} - I_{ws}\Omega\dot{\gamma}\hat{t} \quad (11)$$

Rewriting (11) in a convenient form for the stability proofs we have:

$$J\dot{\omega} = J\omega \times \omega + \mathbf{u} + \mathbf{d} \quad (12)$$

where,

$$\mathbf{u} = -I_{ws}\dot{\Omega}\hat{s} - I_{ws}\Omega\dot{\gamma}\hat{t} \quad (13)$$

where \mathbf{u} contains the control terms $\dot{\Omega}$ and $\dot{\gamma}$ and

$$\mathbf{d} = I_{cg}\dot{\gamma}\omega \times \hat{g} - I_{ws}\Omega\omega \times \hat{s} \quad (14)$$

C. Kinematics and error vector functions for thruster pointing

To define the pointing error kinematics we make use of the Transport theorem [19]. Defining Γ to be the pointing "thruster" vector fixed in the body frame such that $\frac{^B_d}{dt}(\Gamma) = 0$ it follows that:

$$\frac{^N_d}{dt}(\Gamma) = \omega \times \Gamma \quad (15)$$

where ω is the angular velocity of the body frame with respect to the inertial frame. In addition, we define a moving frame D and denote a vector fixed in this frame as Γ_d . It then follows from the Transport Theorem that

$$\frac{^N_d}{dt}(\Gamma_d) = \omega_d \times \Gamma_d \quad (16)$$

where ω_d is the angular velocity of the D frame with respect to the inertial frame. Γ_d defines the desired pointing vector. The pointing vector and the desired angular velocity define the orthonormal frame D .

Usually, as in our rendezvous problem, the reference Γ_d is given, while a feasible ω_d must be computed. The choice of ω_d is not unique for a given Γ_d since ω_d is the angular velocity associated with an orthonormal frame D , with Γ_d a unit vector fixed in that frame. This gives us some flexibility in the choice of ω_d since the frame D can be constructed using Γ_d and an arbitrary, linearly independent, vector.

In this paper ω_d is constructed by taking the cross product of (16) with Γ_d such that:

$$\Gamma_d \times \frac{^N_d}{dt}(\Gamma_d) = \Gamma_d \times (\omega_d \times \Gamma_d) \quad (17)$$

Since Γ_d is a unit vector, then $\|\Gamma_d \times (\omega_d \times \Gamma_d)\| = \|\omega_d\|$. We then choose that $\Gamma_d \times (\omega_d \times \Gamma_d)$ is aligned with ω_d , thus we can define

$$\omega_d = \Gamma_d \times \frac{^N_d}{dt}(\Gamma_d) \quad (18)$$

From the reduced-attitude state (Γ, ω) and the desired reduced-attitude state (Γ_d, ω_d) we define the following error state (Γ_e, ω_e) where the angular velocity error is $\omega_e = \omega - \omega_d$ and the pointing error vector is $\Gamma_e = \Gamma_d \times \Gamma$.

Note that the reduced-attitude control problem does not require ω_3 to be stabilized since the angular velocity vector $\omega = [0 \ 0 \ \omega_3]^T$ is aligned with the pointing axis. Thus, the pointing axis can be asymptotically stabilized for $\omega_3 \neq 0$. Thus, we can consider the reduced angular velocity error $\omega_e^* = \omega_{12} - \omega_{d12}$ where $\omega_{12} = [\omega_1 \ \omega_2 \ 0]^T$ and $\omega_{d12} = [\omega_{d1} \ \omega_{d2} \ 0]^T$. The reduced-attitude control problem using a single VSCMG is then formulated as the problem of designing a feedback law for the control variables $\dot{\gamma}$ and $\dot{\Omega}$ that drives $\omega_e^* \rightarrow 0$ and $\Gamma \rightarrow \Gamma_d$ where $\Gamma_d^O = \frac{\mathbf{a}}{\|\mathbf{a}\|}$ where $\mathbf{a} = f_2(\rho, \rho')$.

III. Nonlinear Control using a single VSCMG

In this section, Lyapunov's direct method and Lasalle's invariance principle [22] are used to develop the nonlinear control laws and prove the stability of the closed-loop system. To aid the stability proofs we note that the error vector function Γ_e is invariant to the choice of basis for Γ and Γ_d . For example, we can define Γ in either the body frame denoted Γ^B or the inertial frame denoted Γ^N . Since $\Gamma^B = A_{B/N} \Gamma^N$ where $A_{B/N}$ is the rotation matrix describing the relative attitude of the two frames and due to the rotational invariance of the cross product, it is straightforward to show that $\Gamma^B \times \Gamma_d^B = \Gamma^N \times \Gamma_d^N$. In addition, $\Gamma \cdot \Gamma_d$ is also independent of the choice of basis, that is, $\Gamma^B \cdot \Gamma_d^B = \Gamma^N \cdot \Gamma_d^N$.

Thus, we can write

$$\frac{d}{dt}(\Gamma_d \cdot \Gamma) = \frac{^N d}{dt}(\Gamma_d^N \cdot \Gamma^N). \quad (19)$$

This enables us to write the following useful relation:

$$\frac{d}{dt}(\Gamma_d \cdot \Gamma) = \omega_e \cdot \Gamma_e \quad (20)$$

This can be shown by the following:

$$\frac{d}{dt}(\Gamma_d \cdot \Gamma) = \frac{^N d}{dt}(\Gamma_d^N \cdot \Gamma^N) = \dot{\Gamma}_d^N \cdot \Gamma^N + \Gamma_d^N \cdot \dot{\Gamma}^N \quad (21)$$

where the dot derivatives in (21) are here used as inertial time derivatives. Then from (15) and (16) we have:

$$\frac{d}{dt}(\Gamma_d \cdot \Gamma) = (\omega_d \times \Gamma_d^N) \cdot \Gamma^N + \Gamma_d^N \cdot (\omega \times \Gamma^N) \quad (22)$$

Using the triple cross product properties this can be expressed as:

$$\frac{d}{dt}(\Gamma_d \cdot \Gamma) = (\Gamma \times \Gamma_d) \cdot \omega_d + \omega \cdot (\Gamma_d \times \Gamma) = \omega_e \cdot \Gamma_e \quad (23)$$

Where in (23) the superscript is omitted due to the invariance of the cross product, meaning that this operation is defined in every basis.

To prove the asymptotic stability of the system, Lyapunov's direct method is used. The theorem in [22] states that, given a Lyapunov function V , if:

- V is continuous and differentiable on all its domain.
- V is positive definite on all its domain.
- \dot{V} is negative definite on all its domain.

Then the system is asymptotically stable. According to Lasalle's principle only the states that explicitly appear in \dot{V} are asymptotically stable and are driven to zero.

To prove the asymptotic stability of the other states, the theorem in [23] is used. This approach evaluates the higher order derivatives of the potential function V when all the states do not appear in the preceding derivative. In particular, a sufficient condition to guarantee asymptotic stability is that the first nonzero higher-order derivative, evaluated on the set of states such that \dot{V} is zero, must be of odd order and be negative definite.

A. Nonlinear reduced-attitude control for thrust-vectoring spacecraft

In the de-tumbling phase of a mission, the control must guarantee the asymptotic stability of the state ω . In other words, when the time $t \rightarrow \infty$, the spacecraft angular velocity $\omega \rightarrow 0$. In [20] the control variables $\dot{\gamma}$ and $\dot{\Omega}$ are chosen to be

$$\dot{\gamma} = k_1 \Omega \omega_t, \dot{\Omega} = k_2 \omega_s \quad (24)$$

Where $\omega_s = \omega^T \hat{s}$ and $\omega_t = \omega^T \hat{t}$ are the projections of the angular velocities on the gimbal frame axes, with k_1 and k_2 positive constants. According to Lyapunov's direct method, this control law ensures that the system is asymptotically stable for the states ω_s and ω_t . According to the definition of ω_s and ω_t , ω_1 and ω_2 will converge to zero. However, ω_3 cannot be controlled to zero. Moreover, as $t \rightarrow \infty$, it will be stabilized to a constant value but, according to LaSalle's principle, it is not guaranteed to asymptotically converge to zero. Since the angular velocities around \hat{b}_1 and \hat{b}_2 can be brought to rest, the pointing axis in the actuator design is chosen to be aligned with \hat{b}_3 . Meaning that the spacecraft body axis \hat{b}_3 can be pointed towards a desired direction, even with a non-zero angular velocity $\omega_3 \neq 0$. In previous work on the reduced-attitude control problem using VSCMG, the pointing axis was constrained to the plane. The assumption that the pointing direction is aligned with the principle axis, enables nonlinear stability proofs for both re-pointing and tracking.

B. Nonlinear control for impulsive thrust-vectoring

For applications to rendezvous using a single impulsive thruster, it is necessary to perform n rest-to-rest attitude maneuvers before each firing. This section develops a rest-to-rest pointing control law using a VSCMG.

The control developed here is fully nonlinear and utilizes a co-ordinate free approach, without the need for Euler angles, quaternions or any other parameterization of SO(3).

Let ω be the angular velocity of the spacecraft expressed in the body frame: $\omega = \omega_1 \hat{b}_1 + \omega_2 \hat{b}_2 + \omega_3 \hat{b}_3$. Note that, only ω_1 and ω_2 are shown to be asymptotically stable and are driven to zero as in the de-tumbling problem described in [20]. As a consequence, the spacecraft will rotate around the pointing direction $\Gamma^B = \hat{b}_3$. In addition we highlight that the angle between Γ and Γ_d must be between $[-\pi ; \pi]$.

The proposed control law is defined by inverting Eq. (13) to get:

$$\dot{\Omega} = -\frac{1}{I_{ws}}(u_1 \cos \gamma + u_2 \sin \gamma) \quad (25)$$

$$\dot{\gamma} = \frac{1}{I_{ws}\Omega}(u_1 \sin \gamma - u_2 \cos \gamma) \quad (26)$$

Where to achieve the pointing stability \mathbf{u} is defined as:

$$\mathbf{u} = [u_1 \ u_2 \ 0]^T = -k_1 \boldsymbol{\omega}_{12} - k_2 \boldsymbol{\Gamma}_e \quad (27)$$

where $\boldsymbol{\omega}_{12} = [\omega_1 \ \omega_2 \ 0]^T$. Expressions (25) and (26) assure that the system is asymptotically stable for the states ω_1 , ω_2 and $\boldsymbol{\Gamma}_e$. In other words, as $t \rightarrow \infty$, $\omega_1 \rightarrow 0$, $\omega_2 \rightarrow 0$, $\boldsymbol{\Gamma}_e \rightarrow 0$.

To prove this, first consider the positive definite Lyapunov function V :

$$V = \frac{1}{2} \boldsymbol{\omega}^T J \boldsymbol{\omega} + k_2 (1 - \boldsymbol{\Gamma}_d \cdot \boldsymbol{\Gamma}), \quad (28)$$

where k_2 is a positive constant. Note that, when the pointing error is zero, the two vectors are aligned such that $\boldsymbol{\Gamma}_d \cdot \boldsymbol{\Gamma} = 1$.

Taking the time derivative of (28) gives

$$\dot{V} = \boldsymbol{\omega}^T (J \dot{\boldsymbol{\omega}} + k_2 (\boldsymbol{\Gamma} \times \boldsymbol{\Gamma}_d)), \quad (29)$$

and using (11) in (29) yields:

$$\dot{V} = \boldsymbol{\omega}^T (J \boldsymbol{\omega} \times \boldsymbol{\omega} - I_{cg} \dot{\gamma} \boldsymbol{\omega} \times \hat{\mathbf{g}} - I_{ws} \Omega \boldsymbol{\omega} \times \hat{\mathbf{s}} - I_{ws} \dot{\Omega} \hat{\mathbf{s}} - I_{ws} \Omega \dot{\gamma} \hat{\mathbf{t}} + k_2 (\boldsymbol{\Gamma} \times \boldsymbol{\Gamma}_d)) \quad (30)$$

From the property of the triple cross product it is clear that:

$$\boldsymbol{\omega}^T (J \boldsymbol{\omega} \times \boldsymbol{\omega}) = 0, \boldsymbol{\omega}^T (I_{cg} \dot{\gamma} \boldsymbol{\omega} \times \hat{\mathbf{g}}) = 0, \boldsymbol{\omega}^T (I_{ws} \Omega \boldsymbol{\omega} \times \hat{\mathbf{s}}) = 0 \quad (31)$$

Then, the expression reduces to:

$$\dot{V} = \boldsymbol{\omega}^T (-I_{ws} \dot{\Omega} \hat{\mathbf{s}} - I_{ws} \Omega \dot{\gamma} \hat{\mathbf{t}} + k_2 (\boldsymbol{\Gamma} \times \boldsymbol{\Gamma}_d)) \quad (32)$$

then from (13) we can write

$$\dot{V} = \boldsymbol{\omega}^T (\mathbf{u} + k_2 \boldsymbol{\Gamma}_e) \quad (33)$$

then substituting (27) into (33) gives:

$$\dot{V} = -k_1 \omega_{12}^2 \quad (34)$$

Equation (34) assures that the system is asymptotically stable for the states ω_1 and ω_2 . While ω_1 and ω_2 will converge to zero, there is no such guarantee on ω_3 . However, since the pointing vector is aligned with the third principal axis of the body frame its direction is invariant to changes in ω_3 . For this reason it is not critical to have stability of ω_3 . However, equation (34) does not show explicit dependence on the state Γ_e . So to prove that the pointing error will converge to zero it is necessary to compute the higher order derivatives of V using the theorem in [23].

To equate (29) and (34) we can set

$$J\dot{\omega} + k_2 \Gamma_e = -k_1 \omega_{12} \quad (35)$$

Then at the equilibrium $\omega_{12} = 0$ (35) becomes

$$\dot{\omega} = -k_2 J^{-1} \Gamma_e \quad (36)$$

Since $\dot{\omega}_3$ must be zero we have $\dot{\omega} = \dot{\omega}_{12}$, then the second and third order derivatives of (34) can be expressed as

$$\ddot{V} = -2k_1 \omega_{12}^T \dot{\omega} \quad (37)$$

$$\ddot{V} = -2k_1 \omega_{12}^T \ddot{\omega} - 2k_1 \dot{\omega}^T \dot{\omega} \quad (38)$$

$$\ddot{V}(\omega_{12} = 0, \dot{\omega} = -k_2 J^{-1} \Gamma_e) = -2k_1 k_2^2 \Gamma_e^2 \quad (39)$$

At $\omega_1 = \omega_2 = 0$ we have $\ddot{V} = 0$ and $\ddot{V} < 0$. Therefore, the system is asymptotically stable and drives $\Gamma_e \rightarrow 0$.

Without loss of generality, it is possible to define Γ_d^B and Γ_e in the following way:

$$\Gamma_d^B = [p_1 \ p_2 \ p_3]^T \quad (40)$$

$$\Gamma_e = \Gamma^B \times \Gamma_d^B = [p_1 \ p_2 \ 0]^T \quad (41)$$

According to (39), as the time $t \rightarrow \infty$, p_1 and p_2 will tend to zero. Then, at the equilibrium (40) becomes:

$$\Gamma_d^B = [0 \ 0 \ p_3]^T \quad (42)$$

Since $\|\Gamma_d\| = 1$, p_3 must be ± 1 . According to Lyapunov's stability conditions on the potential function V , -1 is an

unstable equilibrium point, while +1 is stable. This means that, even if $p_3 = -1$ is a possible solution, any disturbance will cause the movement from the unstable equilibrium point to the stable one, causing the convergence of Γ_d^B to $[0 \ 0 \ 1]^T$, that is the desired state.

C. Nonlinear tracking for low-thrust (continuous) vectoring

Electric propulsion can be used for the purpose of rendezvous and close proximity maneuvers. Such thrusters can provide a small but continuous, throttable, thrust. In the case of using a single electric thruster fixed in the body frame it is possible to provide a continuous force providing its required pointing direction can be continuously matched by the attitude controller. In this case the reduced-attitude control problem becomes one of tracking with a VSCMG.

The proposed tracking VSCMG control law is defined by (25) and (26) with \mathbf{u} defined by:

$$\mathbf{u} = -\mathbf{d}_t^* + J\dot{\omega}_{d12} - k_2\Gamma_e - k_1\omega_e^* \quad (43)$$

This control asymptotically tracks the desired trajectory Γ_d , ω_{d12} assuming that we can measure accurately the disturbance \mathbf{d} . This is because it does not vanish out in the tracking proof as it does in the proof of the pointing stabilization proof. It should be noted that this is a strong assumption since it is dependent on the control variable $\dot{\gamma}$. In practise this term is cancelled using a back-stepping approach where $\dot{\gamma}$ is evaluated using the previous integration time-step. Thus, in practise there will be an error in the estimation of \mathbf{d} which decreases with the integration time step.

where \mathbf{d}_t is the disturbance plus the nonlinear part of the dynamics:

$$\mathbf{d}_t = J\omega \times \omega + \mathbf{d} \quad (44)$$

where $\mathbf{d}_t^* = [d_{t1} \ d_{t2} \ 0]^T$.

Let the candidate Lyapunov function be defined by:

$$V = \frac{1}{2}\omega_e^{*T}J\omega_e^* + k_2(1 - \Gamma_d \cdot \Gamma) \quad (45)$$

Note that this Lyapunov function is only defined on a sub-set of all the states i.e. ω_3 is not included. However, since the pointing direction is invariant to changes in ω_3 it is not required. Using the property (20) the time derivative of V can be expressed as:

$$\dot{V} = \omega_e^{*T}J\dot{\omega}_e^* + k_2(\omega_e \cdot \Gamma_e) \quad (46)$$

Expanding (46):

$$\dot{V} = \omega_e^{*T} (J\dot{\omega}_{12} - J\dot{\omega}_{d12}) + k_2(\omega_e \cdot \Gamma_e) \quad (47)$$

Substituting the system dynamics of (12) in (47):

$$\dot{V} = \omega_e^{*T} (\mathbf{u} + \mathbf{d}_t^* - J\dot{\omega}_{d12}) + k_2(\omega_e \cdot \Gamma_e) \quad (48)$$

Which can be written as:

$$\dot{V} = \omega_e^{*T} (\mathbf{u} + \mathbf{d}_t^* - J\dot{\omega}_{d12} + k_2\Gamma_e) \quad (49)$$

Substituting (43) into (49):

$$\dot{V} = -k_1\omega_e^{*2} \quad (50)$$

Therefore, $\omega_e^* \rightarrow 0$, as $t \rightarrow \infty$.

(50) does not show explicit dependence on the state Γ_e . However, computing the higher order derivatives in an analogous way to the proof of the pointing control it follows that Γ_e will converge to zero as $t \rightarrow 0$.

To obtain an expression as in (50), the closed-loop stability condition is:

$$J\dot{\omega}_e^* + k_2\Gamma_e + k_1\omega_e^* = 0 \quad (51)$$

At the equilibrium, $\omega_e^* = 0$, the condition in (51) is equivalent to:

$$\dot{\omega}_e^* = -k_2 J^{-1} \Gamma_e \quad (52)$$

The higher order derivatives are then:

$$\ddot{V} = -2k_1\omega_e^{*T} \dot{\omega}_e^* \quad (53)$$

$$\ddot{V} = -2k_1\omega_e^{*T} \ddot{\omega}_e^* - 2k_1\dot{\omega}_e^{*T} \dot{\omega}_e^* \quad (54)$$

$$\ddot{V}(\omega_e^* = 0, \dot{\omega}_e^* = -k_2 J^{-1} \Gamma_e) = -2k_1 k_2^2 \Gamma_e^2. \quad (55)$$

The first even order derivative of V , evaluated on the set of states such that \dot{V} is zero, is:

$$\ddot{V}(\omega_e^* = 0) = 0. \quad (56)$$

With the third order derivative negative definite since k_1 and k_2 are positive tuning parameters. Therefore, the control used guarantees that system is asymptotically stable and drives $\Gamma_e \rightarrow 0$.

Differently from the pointing control, ω_{e3} does not converge to a constant. In the pointing case, the potential function was chosen as the total kinetic energy of the system, where both the potential and the potential derivative were functions of all the angular velocity components: $V = V(\omega_1, \omega_2, \omega_3)$ and $\dot{V} = \dot{V}(\omega_1, \omega_2)$. Since both V and \dot{V} satisfy Lyapunov's direct method stability requirements, all angular velocity components are stabilised as $t \rightarrow \infty$. The same cannot be claimed for the tracking control since $V = V(\omega_{e1}, \omega_{e2})$ and $\dot{V} = \dot{V}(\omega_{e1}, \omega_{e2})$, then the only variables that are asymptotically stabilised are ω_{e1} and ω_{e2} . Further analysis is required to characterise the time dependent behaviour of ω_{e3} .

D. Pointing axis angular velocity analysis

It has been shown that the pointing error will converge to the zero vector using the tracking control in the previous subsection. However, the spin around the pointing axis is not proved to be stable in the case of tracking. In this sub-section we provide a simple analysis of the behaviour of ω_3 . This analysis is performed assuming that the inertia matrix is diagonal $J = \text{diag}(I_x, I_y, I_z)$, while the tracking control law yields $\omega_1 \rightarrow \omega_{d1}$ and $\omega_2 \rightarrow \omega_{d2}$, then the rate of change of ω_3 can be expressed as:

$$\dot{\omega}_3 = \frac{I_x - I_y}{I_z} \omega_{d1} \omega_{d2} - \frac{I_{ws}}{I_z} \Omega (\omega_{d1} \sin \gamma - \omega_{d2} \cos \gamma) \quad (57)$$

Note here that in the case of the pointing control (rest-to-rest maneuver) that $\omega_{d1} = \omega_{d2} = 0$ which gives $\dot{\omega}_3 = 0$ and is consistent with the stability proof. For the analysis of the closed-loop system under the tracking control, we rewrite (57) as $\dot{\omega}_3 = n_1 + n_2$ with $n_1 = \frac{I_x - I_y}{I_z} \omega_{d1} \omega_{d2}$ and $n_2 = \frac{I_{ws}}{I_z} \Omega (\omega_{d1} \sin \gamma - \omega_{d2} \cos \gamma)$. The term n_1 is unbounded since ω_{d1} and ω_{d2} could have the same sign, while the term n_2 term is always bounded. Here we provide a simple analysis of ω_3 assuming ω_{d1} and ω_{d2} are slowly time-varying, in which case we assume $\dot{\omega}_{d1} \approx 0$ and $\dot{\omega}_{d2} \approx 0$. Under this assumption n_1 is approximately constant, while n_2 is a term that is time-varying and bounded. In addition, during the tracking task, Ω is in general not constant and varying in time. However, at the equilibrium, $\dot{\Omega}$ is, in general, really small because the control objective is achieved ($\omega_e^* = 0$, $\Gamma_e = 0$) and the controller is only used to compensate for the disturbances of the nonlinear part of the dynamics. However, $\dot{\Omega} \approx 0$ at the equilibrium. As a consequence, Ω is a quasi-static variable and can be considered almost constant.

Using the superposition principle the two contributions n_1 and n_2 can be analysed separately where

$$\dot{\omega}_{3n_1} = n_1 \quad (58)$$

Integrating (58) in time gives:

$$\omega_{3n_1}(t) = \omega_{3n_1}(0) + n_1 t \quad (59)$$

The expression shows that $\omega_{3n_1}(t)$ is secular when $n_1 \neq 0$. This, ω_3 will be driven to its maximum value, constrained by the conservation of the total angular momentum. However, Since $\omega_3 \rightarrow \omega_{3MAX}$, all the angular momentum of the spacecraft will be along the third axis causing saturation of the VSCMG and loss of controllability. To avoid this problem the spacecraft can be designed such that $I_x = I_y$, then $n_1 = 0$. For scenarios where ω_{d1} and ω_{d2} are small, n_1 is a second order term that will not cause the saturation of the VSCMG in practice.

With the obtained condition, (59) becomes:

$$\omega_{3n_1}(t) = \omega_{3n_1}(0) \quad (60)$$

Regarding the second term n_2 ,

$$\dot{\omega}_{3n_2} = -\frac{I_{ws}}{I_z} \Omega (\omega_{d1} \sin \gamma - \omega_{d2} \cos \gamma) \quad (61)$$

Since the right-hand side of (61) is a function of γ , it is possible to write:

$$\omega_{3n_2}(\gamma) = \omega_{3n_2}(0) + \frac{I_{ws}}{I_z} \Omega (\omega_{d1} \cos \gamma + \omega_{d2} \sin \gamma) \quad (62)$$

Using the superposition principle and combining (60) and (62) we have:

$$\omega_3 = \omega_{3n_1} + \omega_{3n_2} = \omega_3(0) + \frac{I_{ws}}{I_z} \Omega (\omega_{d1} \cos \gamma + \omega_{d2} \sin \gamma) \quad (63)$$

ω_3 is, again, a term bounded in time between a maximum and a minimum value.

Assuming for convenience that $\omega_3(0) = 0$, and using typical values such as $\frac{I_{ws}}{I_z} \Omega = 0.07$, $\omega_{d1} = 0.05$, $\omega_{d2} = 0.1$. It is now possible to plot the behaviour of ω_3 for different values of γ .

In Fig.3, ω_3 is plotted against γ where $\gamma \in [-2\pi, 2\pi]$. At the steady state $\dot{\gamma} \approx 0$, thus the value of ω_3 is approximately constant in steady state.

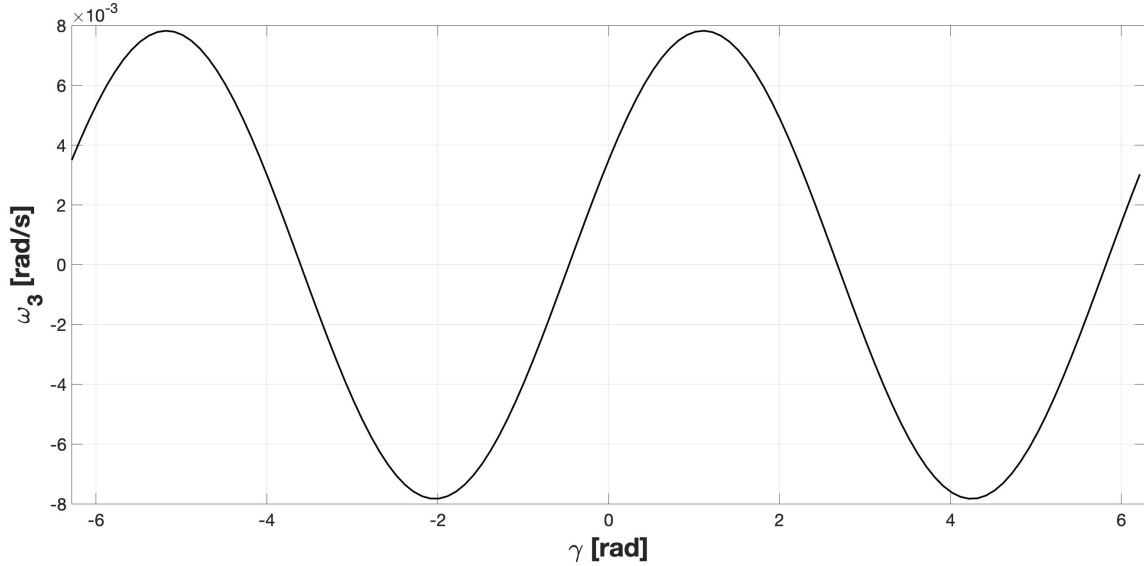


Fig. 3 Third-axis stability.

IV. Simulations

In this section numerical simulations are undertaken for (i) re-pointing a spacecraft from rest to rest, (ii) a rendezvous maneuver and (iii) a rendezvous maneuver with the thruster direction off-set from the centre-of-mass. The inertia properties of the spacecraft are taken from the 12U LUMIO Cubesat [24]. In addition, the orbital equations of motion assume that the chief satellite is on a circular orbit of angular velocity $\dot{\theta}$ where:

$$\ddot{x} - 2\dot{y}\dot{\theta} - 3\dot{\theta}^2x = a_x \quad (64)$$

$$\ddot{y} + 2\dot{\theta}x = a_y \quad (65)$$

$$\ddot{z} + \dot{\theta}^2z = a_z \quad (66)$$

Although more complex dynamics can be used, this simple form is used for simplicity of exposition. In addition, a simple PD control

$$a = -k_3\rho - k_4\dot{\rho} \quad (67)$$

is used to generate the pointing vector $\Gamma_d^N = A_{N/O}\Gamma_d^O$ where $A_{N/O} = A_{O/N}^T$

$$A_{N/O} = \begin{bmatrix} \cos \theta & \sin \theta & 0 \\ -\sin \theta & \cos \theta & 0 \\ 0 & 0 & 1 \end{bmatrix} \quad (68)$$

A. Repointing towards an inertially fixed direction

Results of the numerical simulations for re-pointing the conceptual CubeSat are shown in this sub-section.

Table 1 Repointing: simulation data

Symbol	Meaning	Value	Measure Unit
ω_0	S/C initial angular velocity	[0 0 0.15]	$\frac{\text{rad}}{\text{s}}$
$[\Gamma_{d0}]^B$	Initial desired attitude in body frame	$\left[\frac{1}{\sqrt{3}} \frac{1}{\sqrt{3}} \frac{1}{\sqrt{3}} \right]$	-
$[I_x I_y I_z]$	S/C inertias	$[100.9 \ 25.1 \ 91.6] \times 10^{-2}$	$\text{kg} \cdot \text{m}^2$
$[I_{cg} I_{ws}]$	VSCMG inertias	[0.002 0.03]	$\text{kg} \cdot \text{m}^2$
Ω_0	Wheel angular velocity	1	$\frac{\text{rad}}{\text{s}}$
γ_0	Initial gimbal angle	1	$\frac{\text{rad}}{\text{s}}$
k_1	Control parameter 1	0.5	-
k_2	Control parameter 2	0.5	-

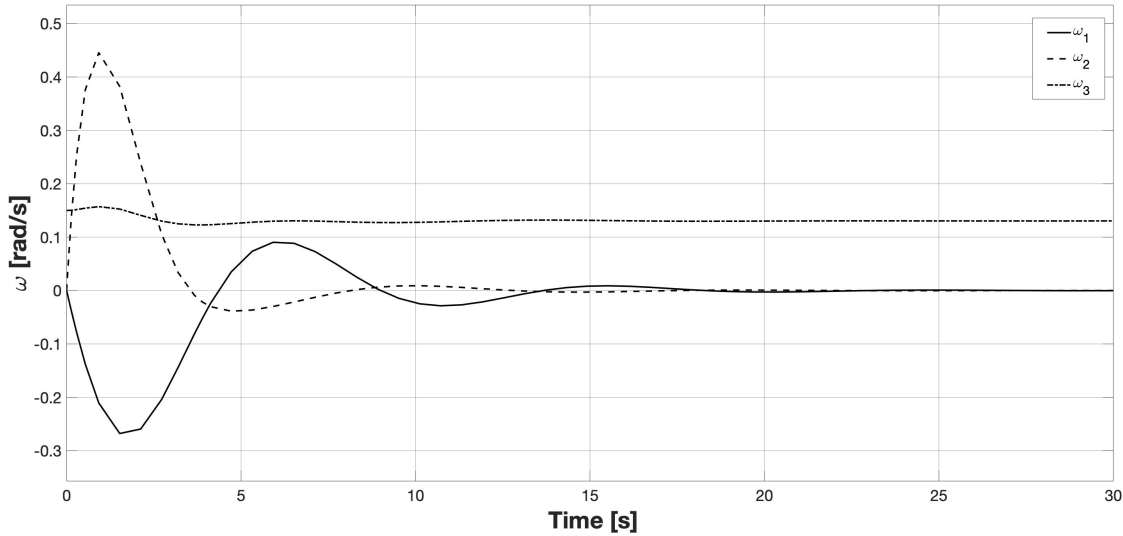


Fig. 4 Repointing: angular velocity.

In fig.4, the angular velocities ω_1 and ω_2 asymptotically converge to zero, while ω_3 is asymptotically stabilized to a constant value in agreement with our theoretical analysis. In fig.5, the desired pointing direction Γ_d , in the body frame, is plotted against time. We can see that the re-pointing maneuver takes approximately 30 seconds and at the equilibrium

Γ_d is aligned with \hat{b}_3 .

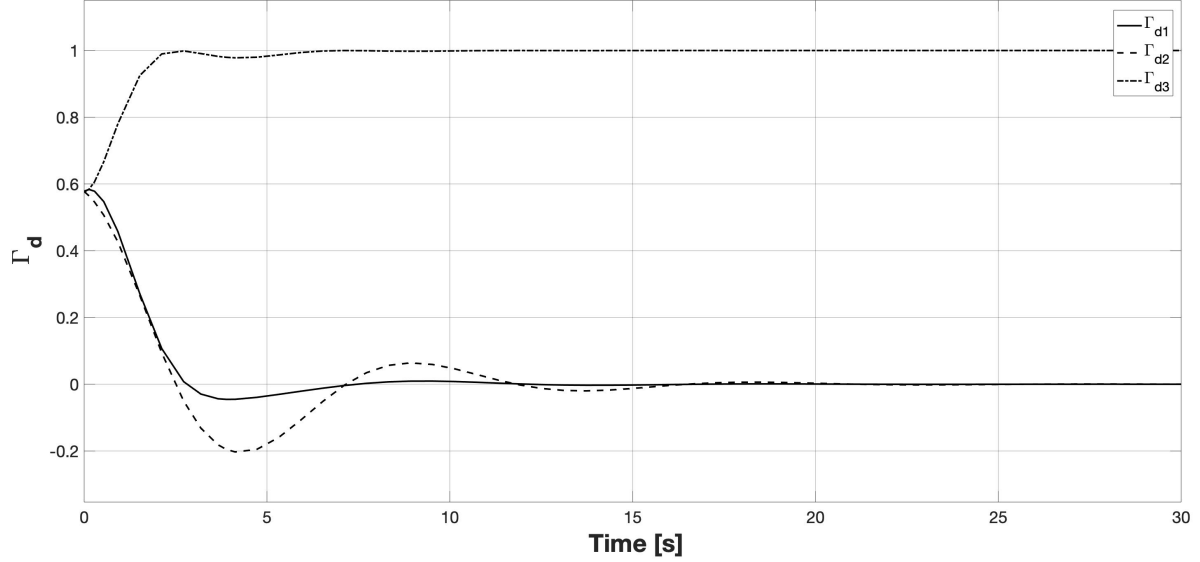


Fig. 5 Pointing: desired attitude

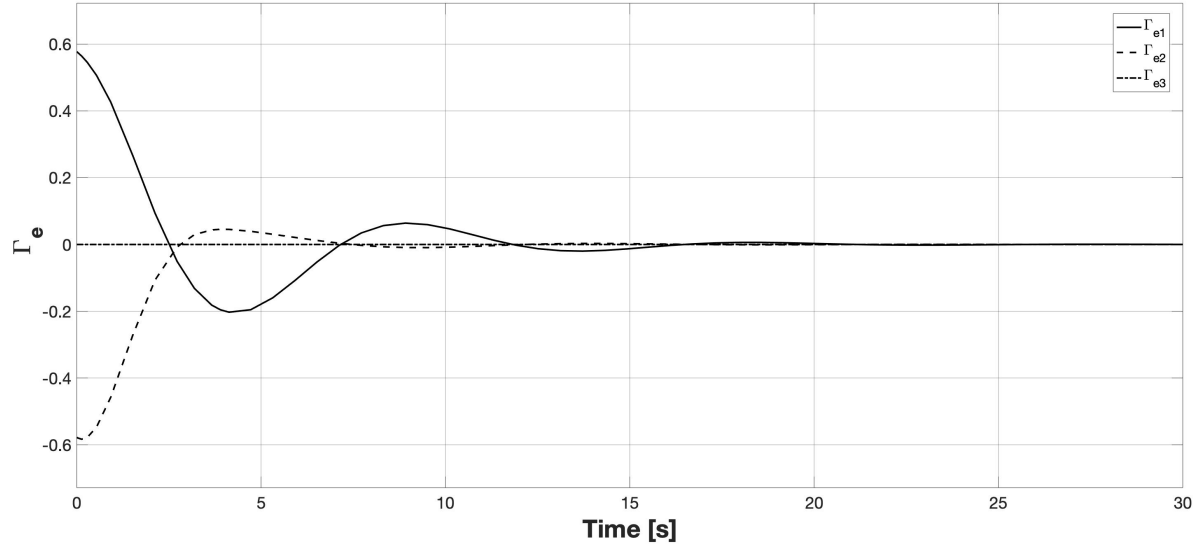


Fig. 6 Pointing: attitude error

B. Tracking of a time-varying reference direction

Fig.7 shows that ω_1 and ω_2 asymptotically converge to zero, while ω_3 is characterized by an oscillatory steady-state behaviour shown in fig.8, in agreement with the analysis in (63).

In fig.9, the desired attitude Γ_d is represented, showing that the tracking task objective is successfully achieved in approximately 900 seconds.

Table 2 Tracking: simulation data

Symbol	Meaning	Value	Measure Unit
ω_0	S/C initial angular velocity	[0 0 0.15]	$\frac{rad}{s}$
$[\Gamma_d(t)]^N$	Desired attitude in inertial frame	[0 $\sin(0.2t)$ $\cos(0.2t)$]	-
$[I_x I_y I_z]$	S/C inertias	$[100.9 \ 25.1 \ 91.6] \times 10^{-2}$	$kg \cdot m^2$
$[I_{cg} I_{ws}]$	VSCMG inertias	[0.002 0.03]	$kg \cdot m^2$
Ω_0	Wheel angular velocity	1	$\frac{rad}{s}$
γ_0	Initial gimbal angle	1	$\frac{rad}{s}$
k_1	Control parameter 1	0.1	-
k_2	Control parameter 2	0.1	-

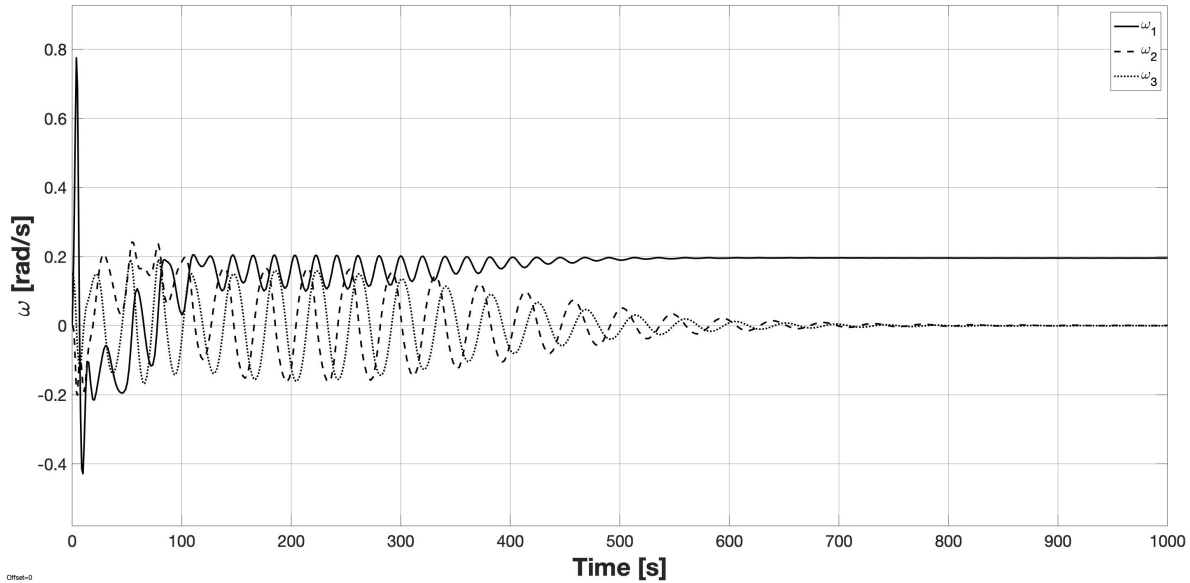


Fig. 7 Tracking: angular velocity.

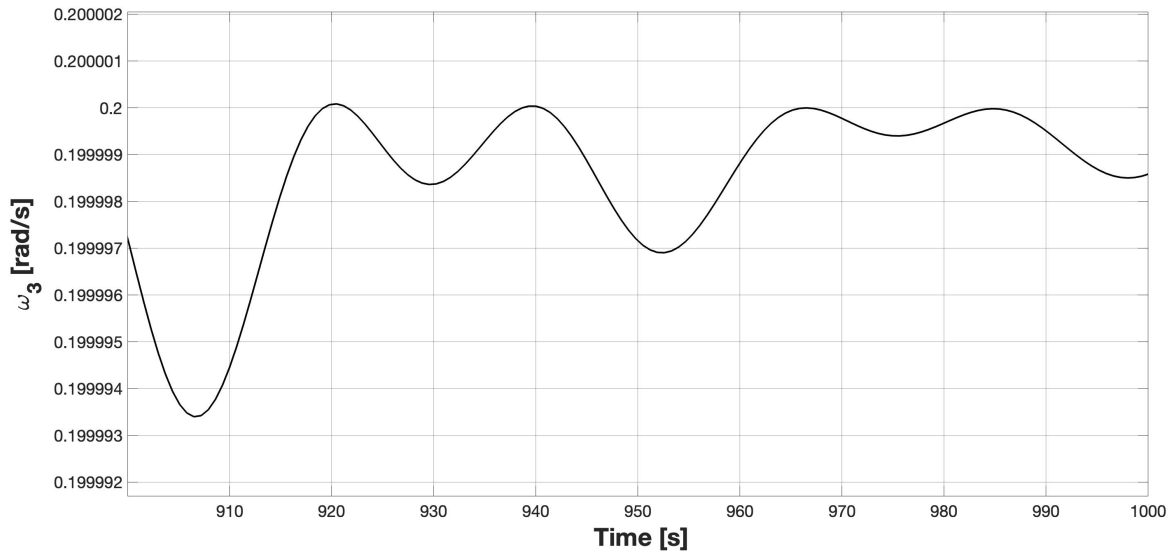


Fig. 8 Tracking: ω_3 steady-state behaviour

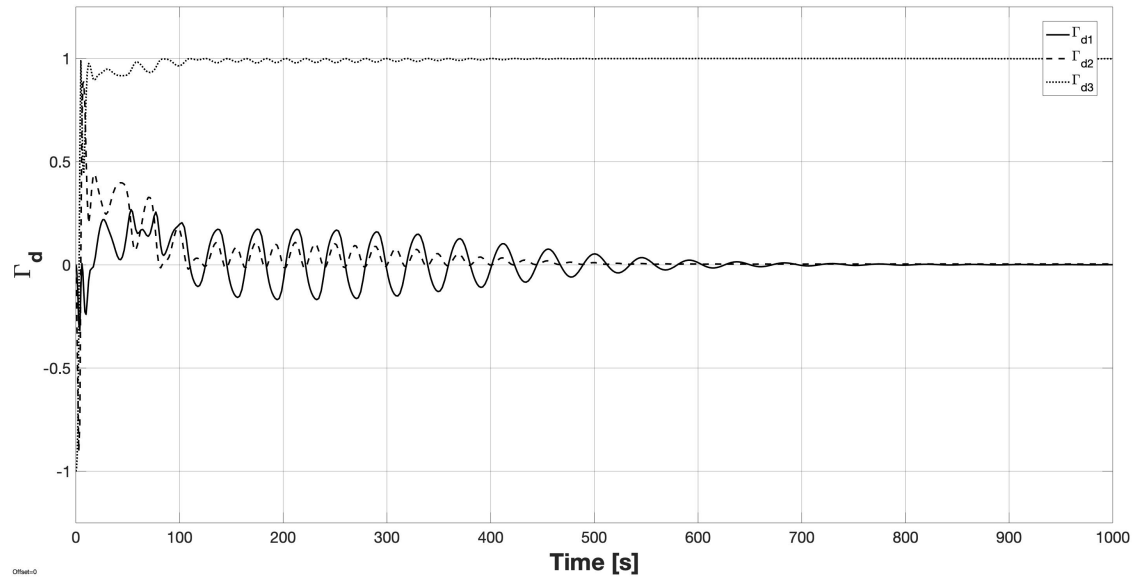


Fig. 9 Tracking: desired attitude.

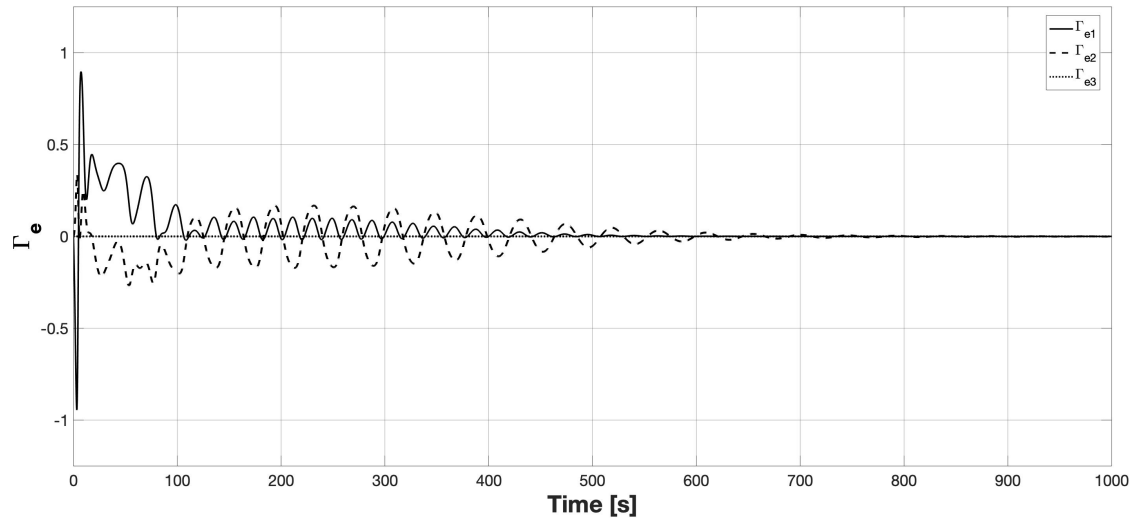


Fig. 10 Tracking: attitude error.

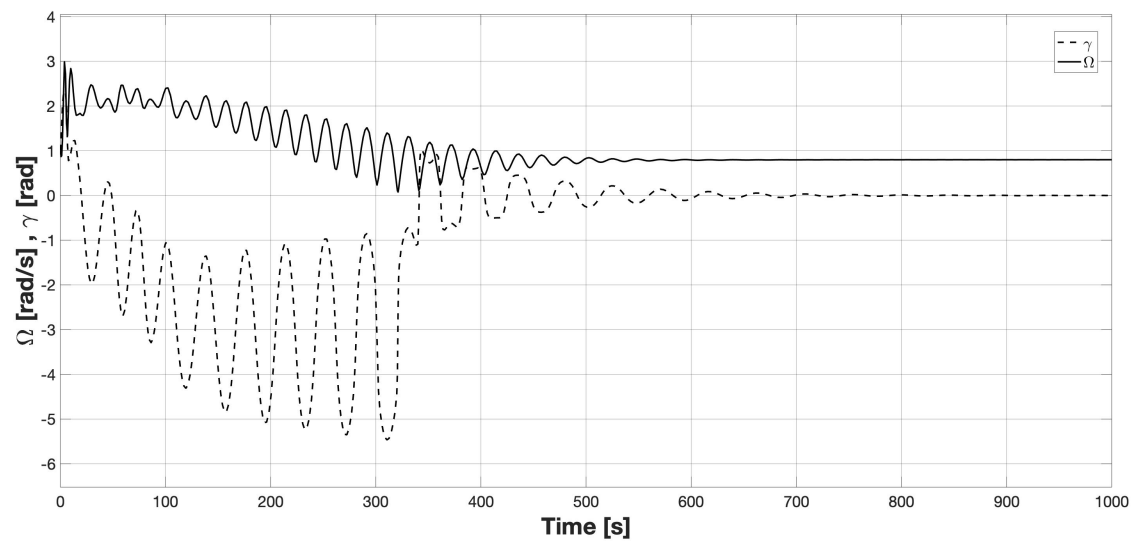


Fig. 11 Tracking: Ω and γ .

In fig.11, the wheel angular velocity Ω and the gimbal angle γ are shown to be bounded to relatively small values once they reach the equilibrium. Figures 12 and 13, show the quasi-static steady-state nature of the variables Ω and γ .

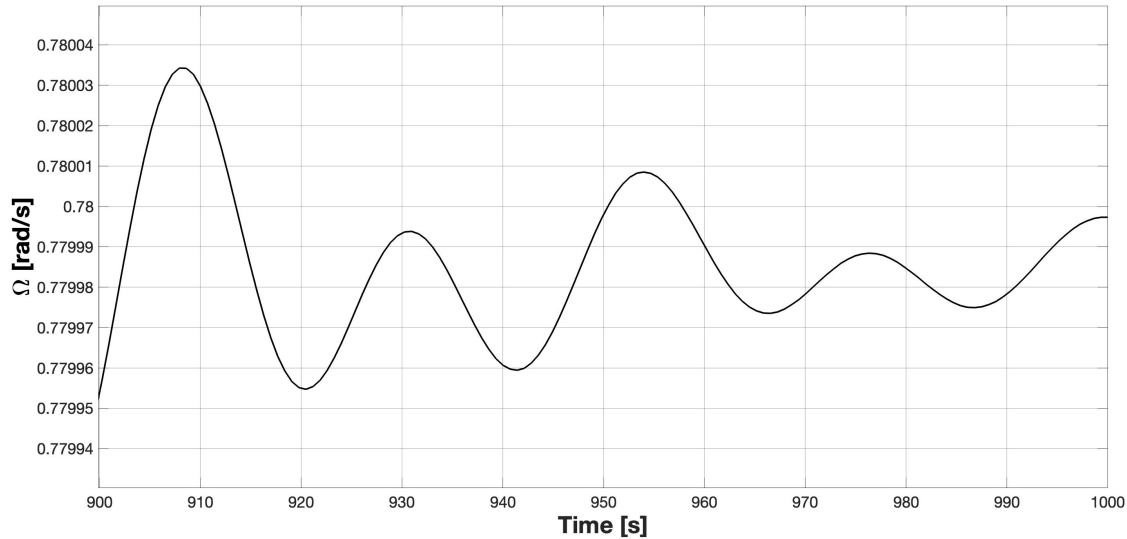


Fig. 12 Tracking: Ω steady-state behaviour.

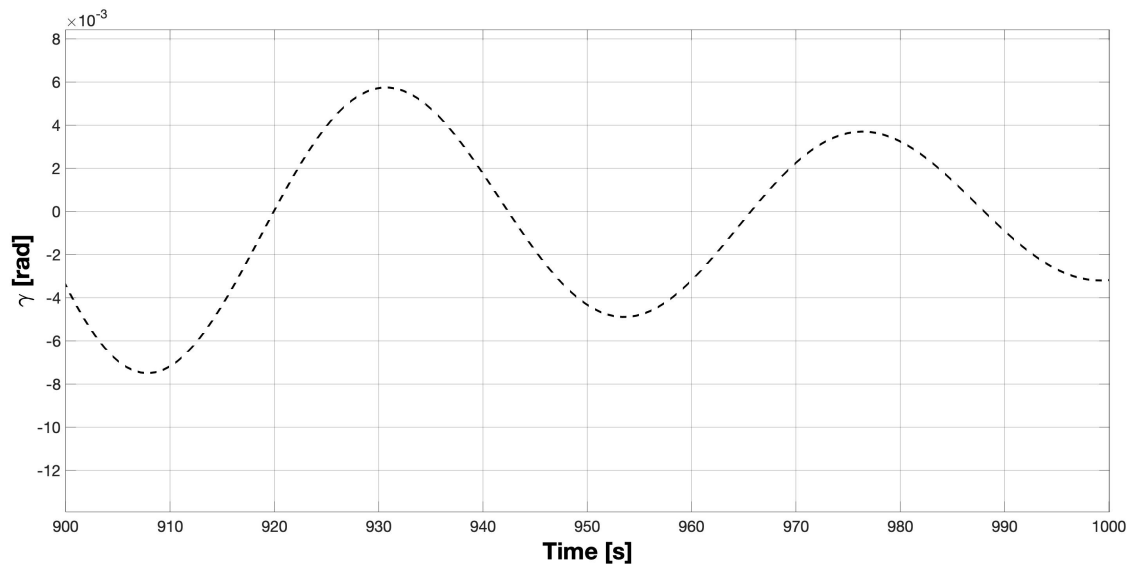


Fig. 13 Tracking: γ steady-state behaviour.

C. Rendezvous

The rendezvous manoeuvre, schematized in fig.14, is successfully performed, bringing the chief satellite to the target, as shown in fig.15 where the relative distances are plotted. The required acceleration module, shown in fig.16, is limited to very small values, making this kind of manoeuvre suitable even for systems equipped with low-thrust capability.

Table 3 Rendezvous: simulation data

Symbol	Meaning	Value	Measure Unit
ω_0	S/C initial angular velocity	[0.1 0.1 0.1]	$\frac{rad}{s}$
$[I_x I_y I_z]$	S/C inertias	$[100.9 \ 25.1 \ 91.6] \times 10^{-2}$	$kg \cdot m^2$
$[I_{cg} I_{ws}]$	VSCMG inertias	[0.002 0.03]	$kg \cdot m^2$
Ω_0	Wheel angular velocity	1	$\frac{rad}{s}$
γ_0	Initial gimbal angle	1	$\frac{rad}{s}$
r_0	Chief satellite initial position in inertial frame	[9900 0 0]	Km
r_{t0}	Target satellite initial position in inertial frame	[9998.47 174.52 0]	Km
v_0	Chief satellite initial velocity in inertial frame	[0 6.345 0]	$\frac{Km}{s}$
v_{0t}	Target satellite initial velocity in inertial frame	[-0.110 6.312 0]	$\frac{Km}{s}$
k_1	Control parameter 1	0.5	-
k_2	Control parameter 2	0.5	-
k_3	Control parameter 3	0.0005	-
k_4	Control parameter 4	0.05	-

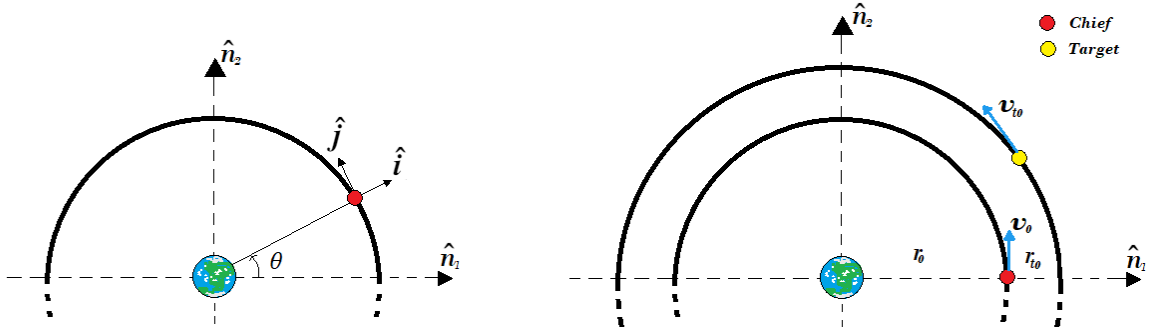


Fig. 14 Problem scheme.

Figures 17 and 18 show the spacecraft angular velocity and attitude evolution converge after approximately 800 seconds. The control torques in Fig.20 suggest that the VSCMG is fully capable of performing this maneuver without saturating. Fig.20 also shows that the values assumed by $\dot{\gamma}$ and $\dot{\Omega}$ are bounded between similar values, meaning that the control is equally distributed along both axes. In general, $\dot{\Omega}$ will tend to assume larger values than $\dot{\gamma}$ because on the \hat{s} axis, where the VSCMG works like a RW, the torque generated does not benefit of the amplification effect typical of CMGs.

Finally, a tridimensional representation of the manoeuvre is given in fig.21.

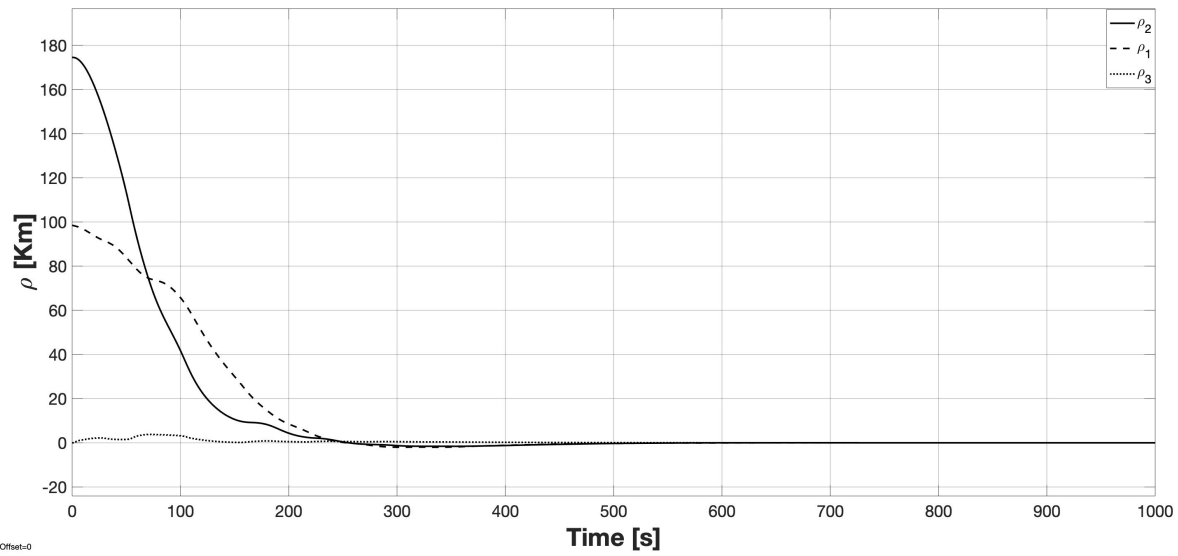


Fig. 15 Rendezvous: relative distances.

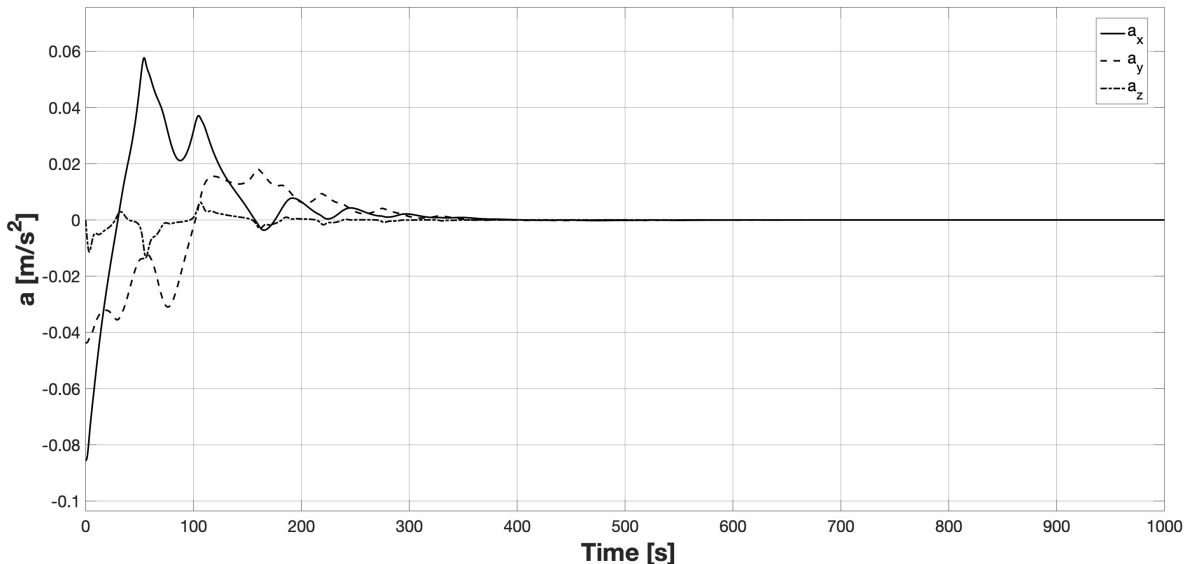


Fig. 16 Rendezvous: thruster acceleration.

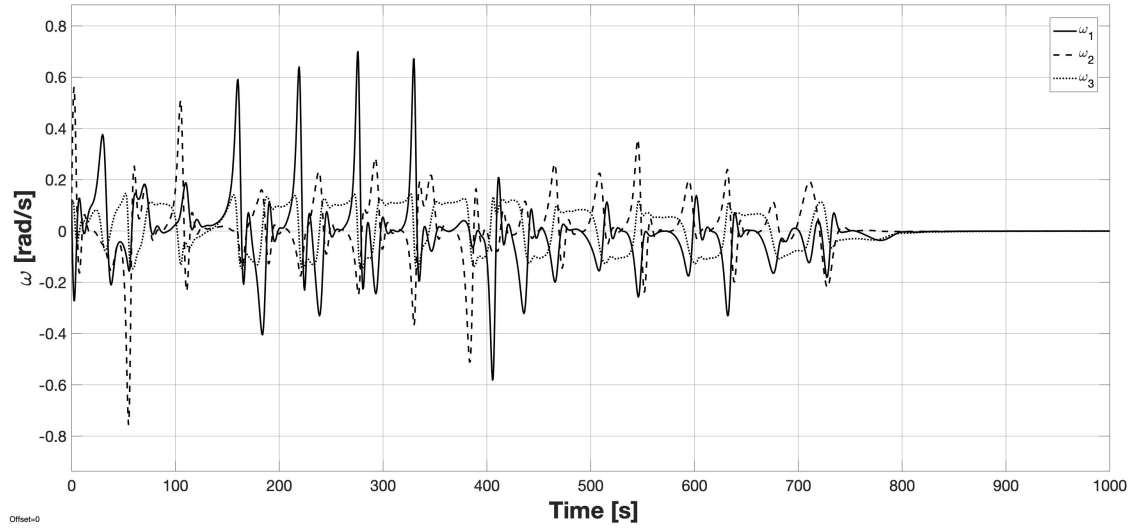


Fig. 17 Rendezvous: S/C angular velocity.

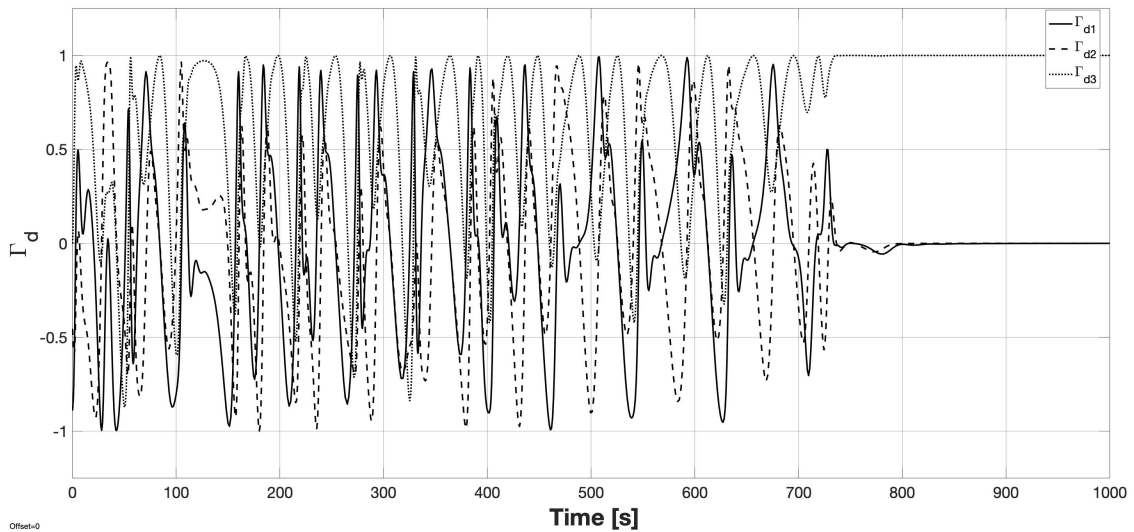


Fig. 18 Rendezvous: desired attitude.

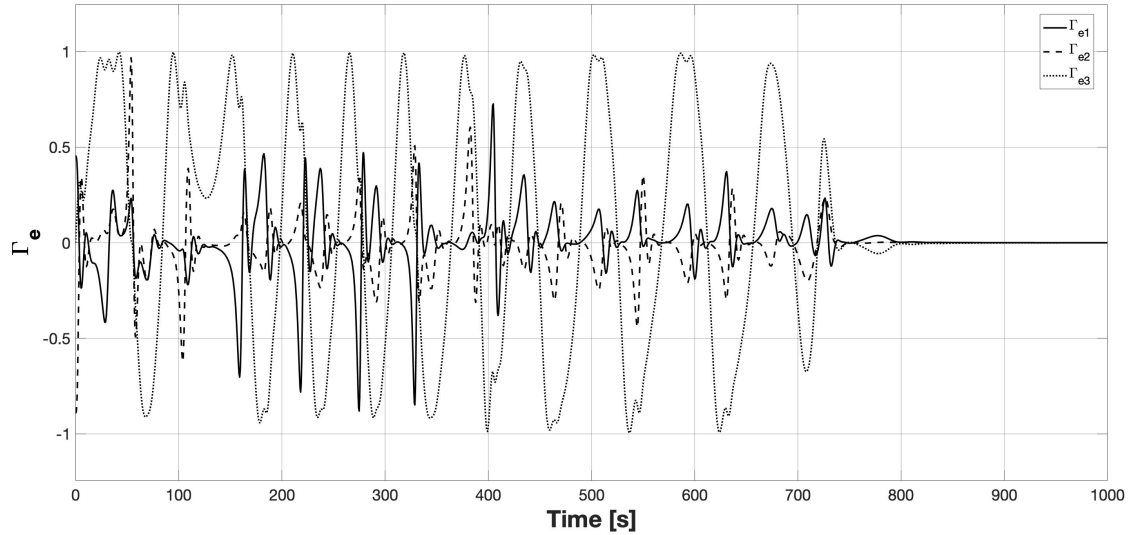


Fig. 19 Rendezvous: attitude error.

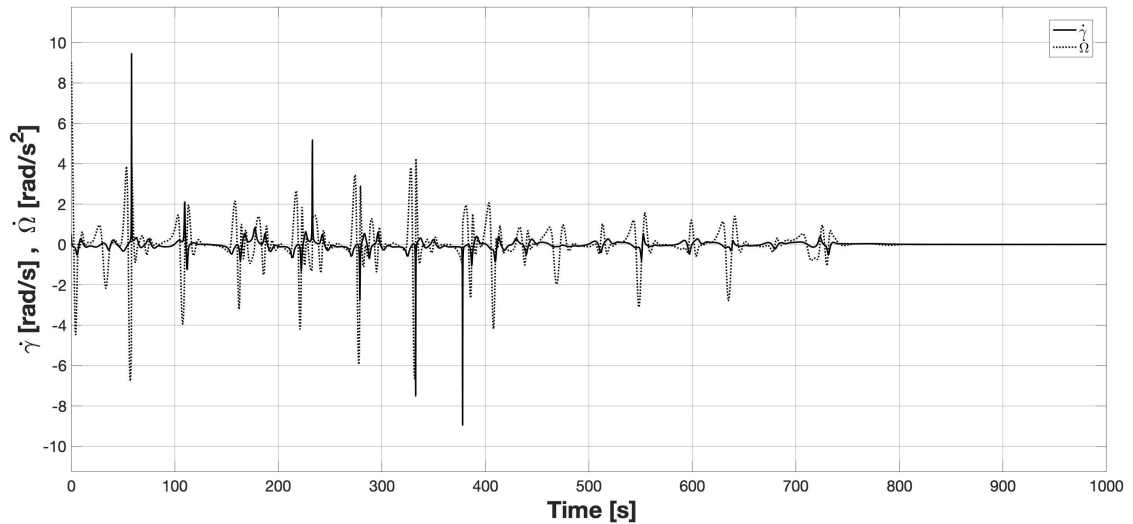


Fig. 20 Rendezvous: control variables.

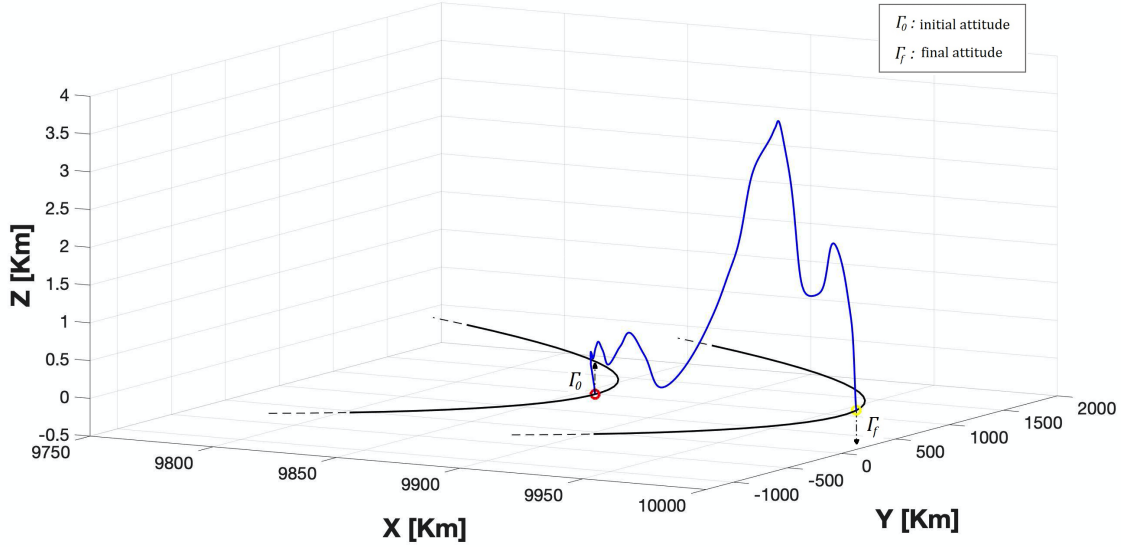


Fig. 21 Rendezvous: manoeuvre 3D visualisation.

D. Effect of an off-set thruster on the rendezvous manoeuvre

In the previous simulation it was assumed that the thruster was perfectly aligned with the spacecraft center-of-mass. This scenario is not likely in reality where a small misalignment is always present and can produce undesired torques.

In Fig.22 the thruster off-set is illustrated. The misalignment of the thruster produces two parasitic torques on the principal axes \hat{b}_1 and \hat{b}_2 . In this analysis a disturbance on $(\hat{b})_3$ is not considered. Such a deviation of the thrust direction could be due to imperfections in the nozzle of a chemical thruster and does not occur in electric thrusters. However, this detail is not considered in this analysis.

$$m_{t1} = \|\mathbf{T}\| d_1 = m_{s/c} \|\mathbf{a}\| d_1 \quad (69)$$

$$m_{t2} = \|\mathbf{T}\| d_1 = m_{s/c} \|\mathbf{a}\| d_2 \quad (70)$$

Starting from these two components we can define a disturbance torque due to the off-set as:

$$\mathbf{m}_t = [m_{t1} \ m_{t2} \ 0]^T \quad (71)$$

Rewriting (12) including this term gives:

$$J\dot{\omega} = J\omega \times \omega + \mathbf{u} + \mathbf{d} + \mathbf{m}_t \quad (72)$$

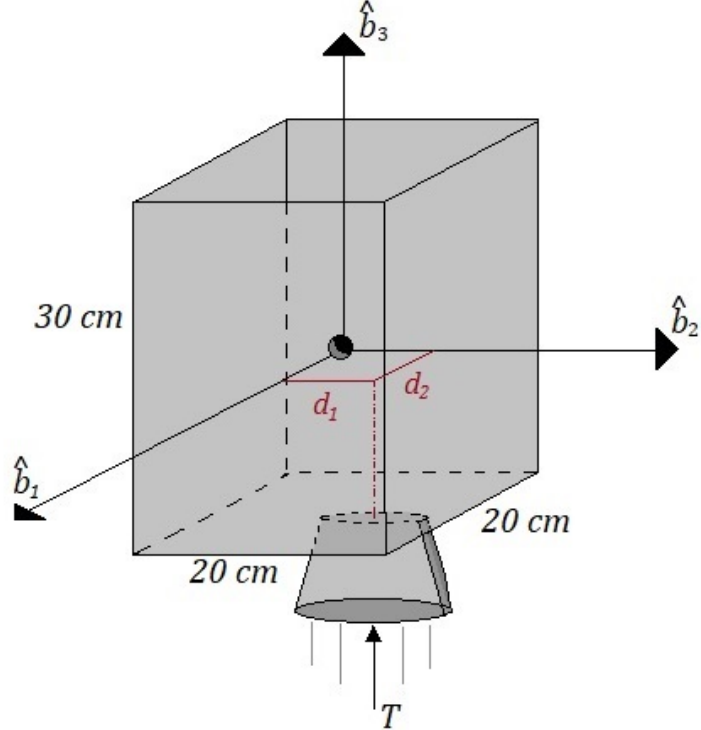


Fig. 22 CubeSat with off-set thruster.

In the data reported in Table 3, we add the mass of the LUMIO Cubesat [24] along with the misalignments d_1 and d_2 that are chosen as 5% of the length of their respective sides.

Table 4 Rendezvous with off-set thruster: additional data

Symbol	Meaning	Value	Measure Unit
$m_{s/c}$	S/C mass	23.82	Kg
d_1	off-set on \hat{b}_1	0.01	m
d_2	off-set on \hat{b}_2	0.01	m

From the figures it is shown that the mission objective is successfully achieved even when the thruster is off-set from the centre-of-mass. However, from figures 25, 26, 27 we can see that the manoeuvre takes a longer time to reach the equilibrium, approximately 2800 seconds.

Comparing the control variables in Fig.28 with the ones in Fig.20, it can be seen that overall the manoeuvre requires more control to counteract the parasitic torque during the mission. However the values for $\dot{\gamma}$ and $\dot{\Omega}$ remain bounded and of the same magnitude of order, indicating that, for reasonable misalignments of the thruster, the contribution of \mathbf{m}_t will not saturate the VSCMG.

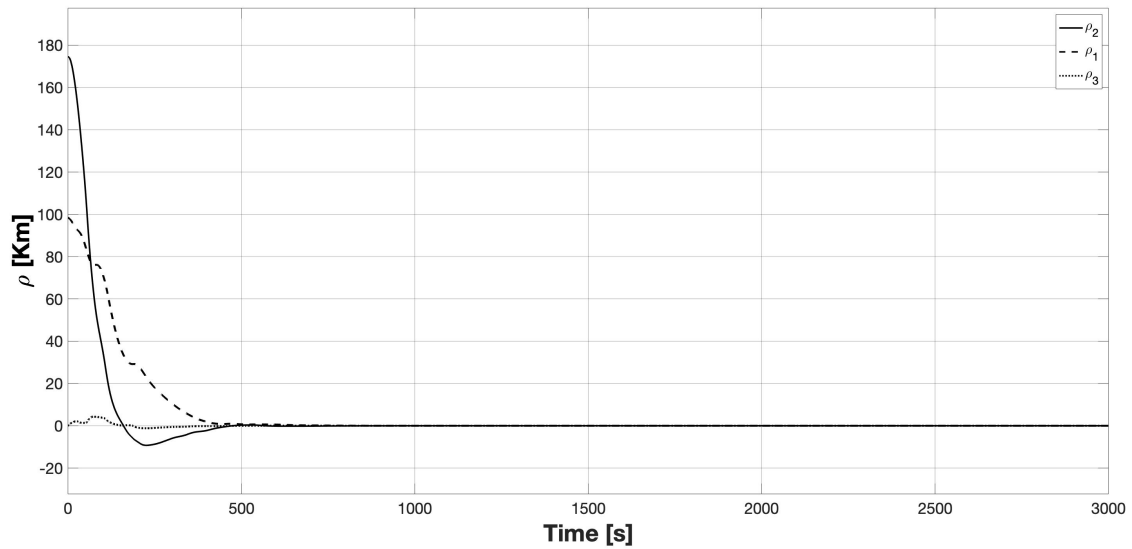


Fig. 23 Rendezvous with off-set thruster: relative distances.

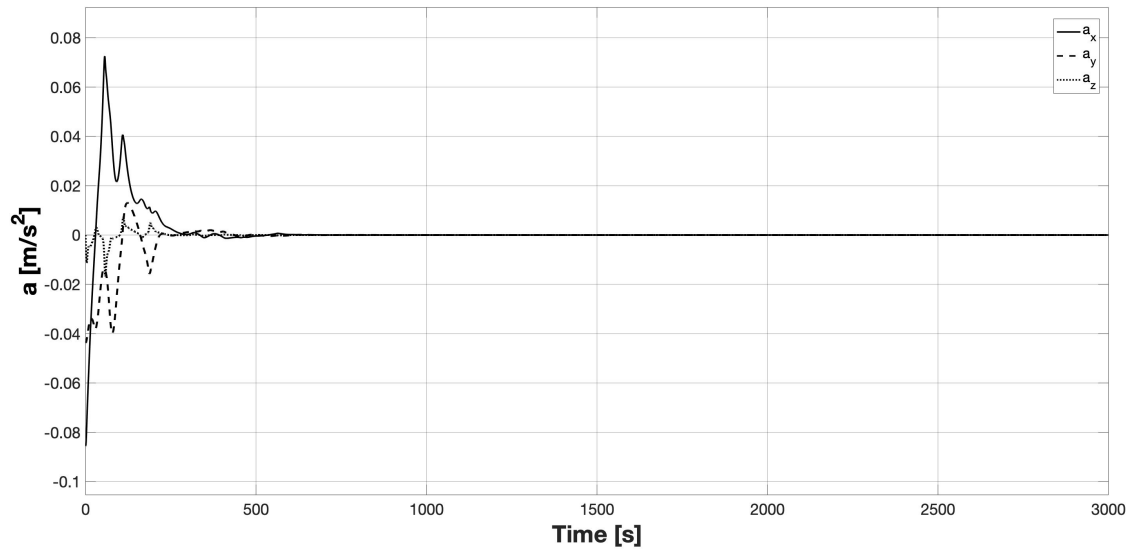


Fig. 24 Rendezvous with off-set thruster: thruster acceleration.

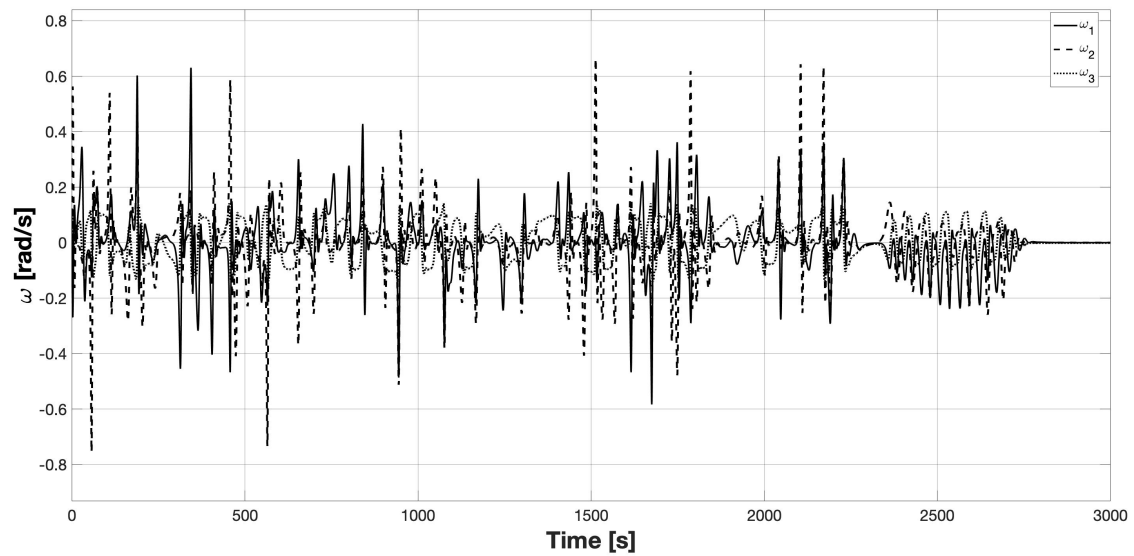


Fig. 25 Rendezvous with off-set thruster: S/C angular velocity.

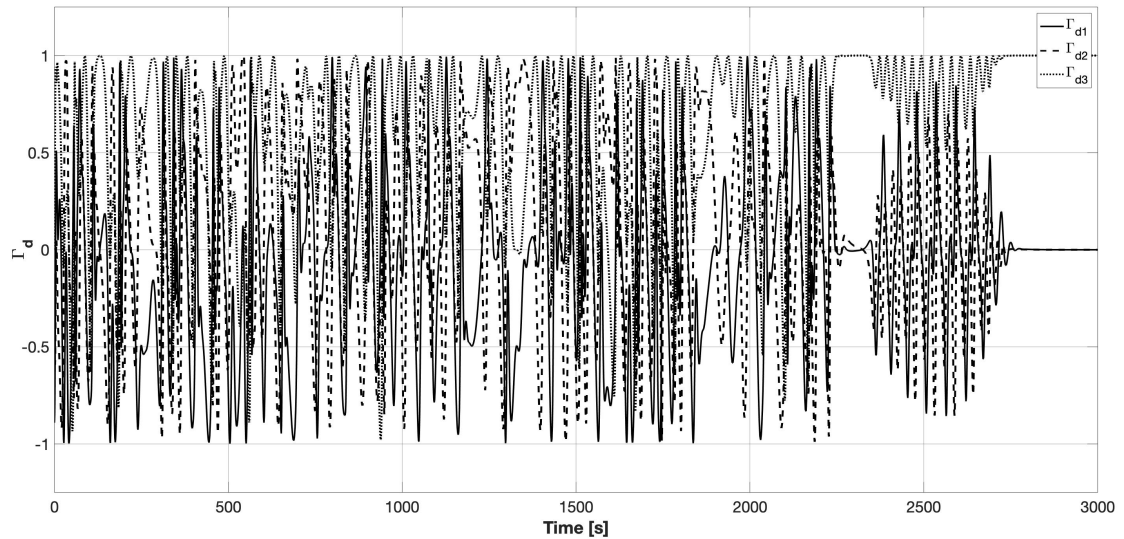


Fig. 26 Rendezvous with off-set thruster: desired attitude.

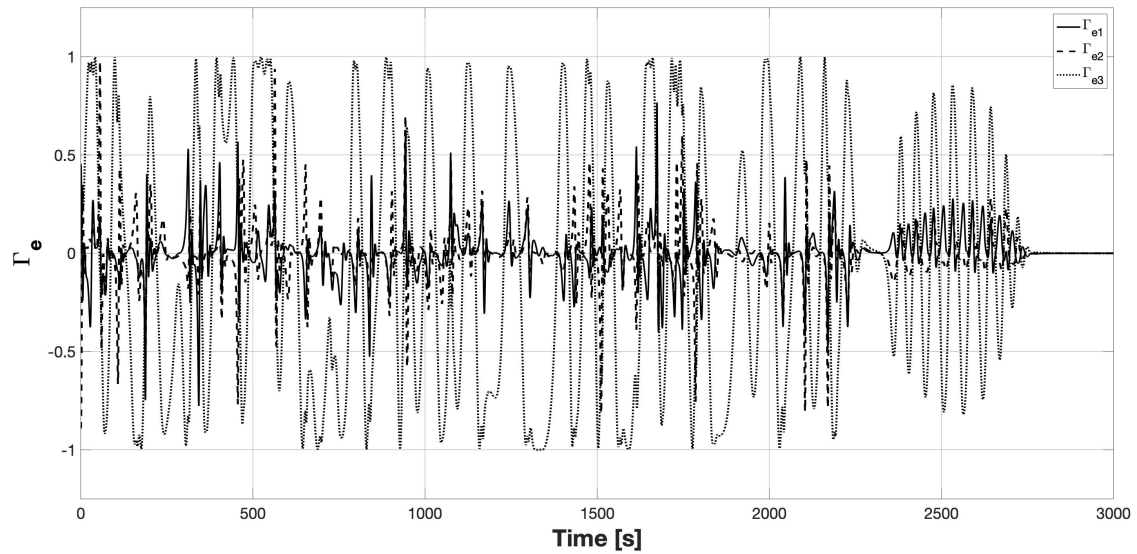


Fig. 27 Rendezvous with off-set thruster: attitude error.

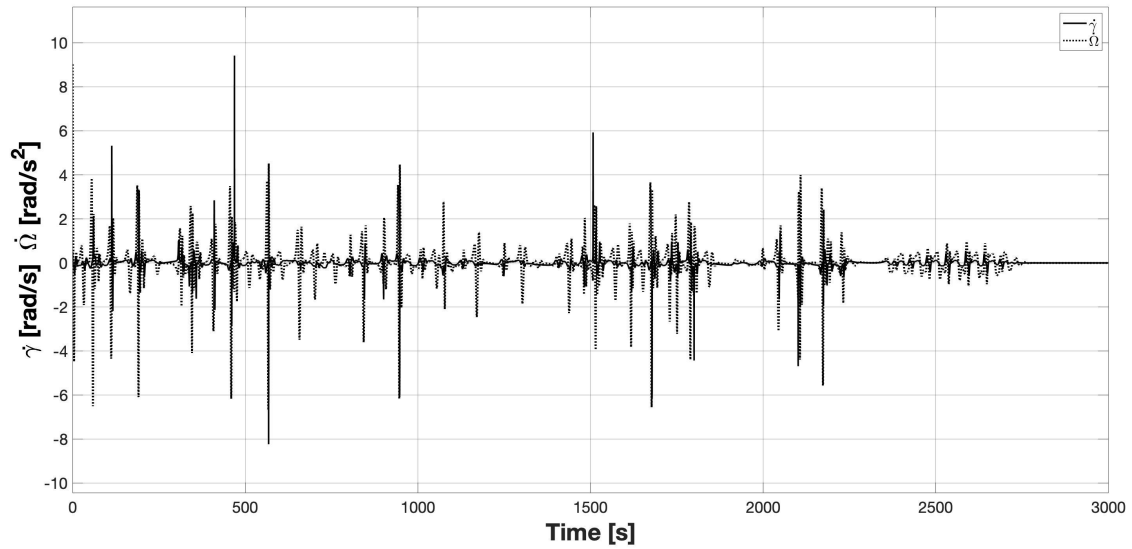


Fig. 28 Rendezvous with off-set thruster: control variables.

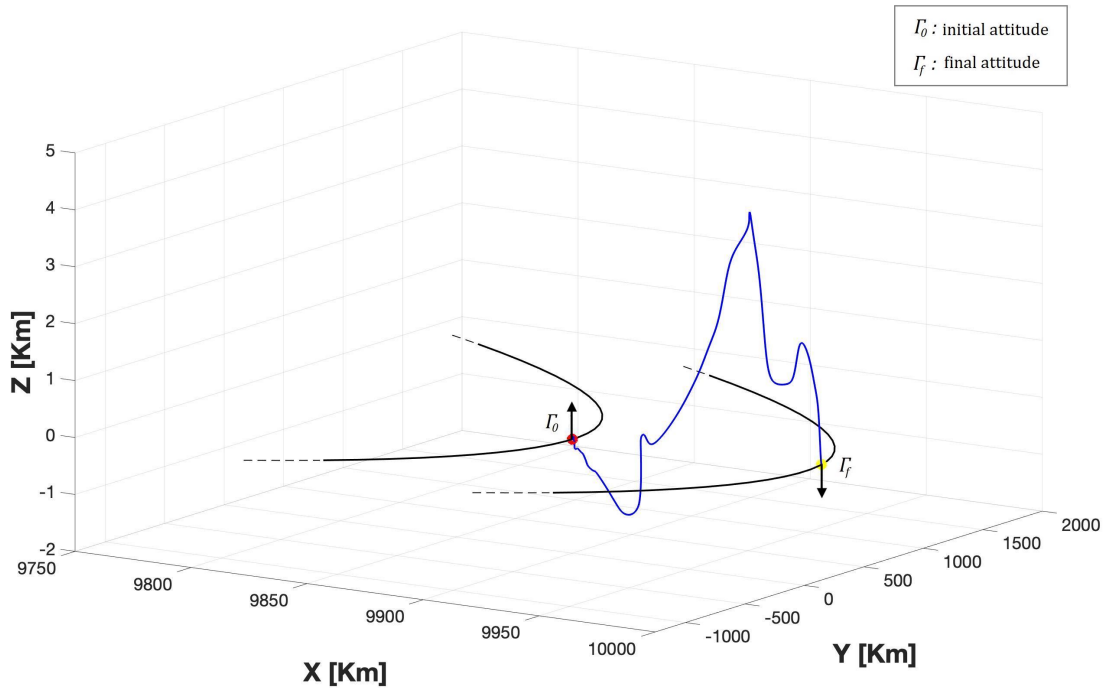


Fig. 29 Rendezvous with off-set thruster: manoeuvre 3D visualisation.

V. Conclusion

In this paper, an actuator configuration using only a single thruster and momentum exchange device was proposed for rendezvous and docking. This design is enabled by considering the reduced-attitude control problem where control of the angular velocity around the pointing axis is not considered as a requirement. Nonlinear control laws were proposed for rest-to-rest pointing, and tracking where the closed-loop system was proved asymptotically stable using Lyapunov's direct method (although the angular velocity stability about the pointing axis is not proved). Moreover, it was shown that spacecraft asymmetry does not compromise the system asymptotic stability in the case of pointing with respect to a fixed inertial frame, while imposing the symmetry of the spacecraft around the pointing axis, was required to prove tracking.

These control laws could enable high-maneuverability of a thrust-vectoring CubeSat utilizing either a single cold-gas thruster (impulsive) or an electric propulsion thruster (continuous). To demonstrate this, the derived control laws were applied to a practical rendezvous problem, where a 12U CubeSat, provided with only one body-fixed thruster and one Variable Speed Control Moment Gyro (VSCMG) for thrust-vectoring, needs to be brought in proximity of a target. This paper proposes a fully nonlinear, nonsingular control law for tracking of a time-varying pointing reference, for the first time, using a VSCMG. The control laws can be useful in missions where only two-axis stabilization is of interest (e.g., the line-of-sight direction of a camera or antenna). This type of spacecraft could potentially also be used for rendezvous and docking. However, since the thruster axis can have a rotation about this would be problematic for docking. However, the docking mechanism could be of screw-in type, in which case pointing would have to be very accurate. Alternatively,

in the final stage an additional actuator such as a small reaction wheel could be used to bring this axis to rest.

The use of a single thruster and VSCMG for orbit-attitude control may be useful for the design of Cubesats utilizing as few actuators as possible in order to minimize mass. In addition, the controls of this paper could be used to mitigate actuator failure. For example, if this VSCMG is paired with other actuators for 3-axis control, then in the event of failure of these actuators the VSCMG can still maintain control of the pointing axis.

Future work will focus on the development of robust thrust-vectoring control using a VSCMG. Robustness to external disturbances, thruster mis-firing, actuator faults as well as thruster misalignment with the centre-of-mass is essential if such a conceptual CubeSat is to be realized in future missions.

References

- [1] Zhang, J., Biggs, J. D., Ye, D., and Sun Z., "Finite-time attitude set-point tracking for thrust-vectoring spacecraft rendezvous", Aerospace Science and Technology 96, 105588, 2019, pp. 1-10. <https://doi.org/10.1016/j.ast.2019.105588>
- [2] Schaub, H., Vadali, S. R., and Junkins, J. L., "Feedback Control Law for Variable Speed Control Moment Gyroscopes", Journal of the Astronautical Sciences, Vol. 45, No. 3, 1998, pp. 307-328.
- [3] Chaturvedi, N. A., Sanyal, A. K., and McClamroch, N. H., "Rigid-Body Attitude Control", IEEE Control Systems Magazine, vol. 31, no. 3, 2011, pp. 30-51. <https://doi.org/10.1109/MCS.2011.940459>
- [4] Geng, Y., Li, C., Guo, Y., and Biggs, J.D., "Fixed-time near-optimal control for repointing maneuvers of a spacecraft with nonlinear terminal constraints", ISA Transactions, 2019, pp. 1-13. <https://doi.org/10.1016/j.isatra.2019.07.026>
- [5] Chabot, J., Schaub, H., "Spherical magnetic dipole actuator for spacecraft attitude control", Journal of Guidance, Control, and Dynamics, Vol. 39, No. 4, 2016, pp. 911-915. <https://doi.org/10.2514/1.G001471>
- [6] Patankar, K., and Fitz-Coy, N., "A Hybrid CMG-RW Attitude Control Strategy for Agile Small Satellites", Advances in the Astronautical Sciences, Vol. 150, 2014, pp. 2057-2066.
- [7] Cornick, E. D., "Singularity Avoidance Control Laws for Single Gimbal Control Moment Gyros", Proceedings of the AIAA guidance and control conference, 1979, pp. 20-33. <https://doi.org/10.2514/6.1979-1698>
- [8] Margulies, G., and Aubrun, J.N., "Geometric theory of single-gimbal control moment gyro systems", Journal of the astronomical sciences, Vol.26, No.2, 1978, pp. 159-191.
- [9] Ismail, Z., and Varatharajoo, R., "A study of reaction wheel configurations for a 3-axis satellite attitude control", Advances in space research, Vol.45, Issue 6, 2010, pp. 750-759. <https://doi.org/10.1016/j.asr.2009.11.004>
- [10] Votel, R., and Sinclair, D. , "Comparison of Control Moment Gyros and Reaction Wheels for Small Earth-Observing Satellites", 26th annual AIAA/USU conference on small satellites, SSC12-X-1, 2012. pp. 1-6.

- [11] Horri, N.M., and Palmer, P., "Practical Implementation of Attitude-Control Algorithms for an Underactuated Satellite", Journal of guidance, control, and dynamics, Vol.35, No.1, 2012, pp. 40-43. <https://doi.org/10.2514/1.54075>
- [12] Biggs, J.D., and Bai, Y., Henninger H., "Attitude guidance and tracking for spacecraft with two reaction wheels", International Journal of Control, Vol. 91, Issue 4, 2018, pp. 926-936. <https://doi.org/10.1080/00207179.2017.1299944>
- [13] Tsotras, P., and Luo, J., "Control of underactuated spacecraft with bounded inputs", Automatica Vol. 36, Issue 8, 2000, pp. 1153-1169. [https://doi.org/10.1016/S0005-1098\(00\)00025-X](https://doi.org/10.1016/S0005-1098(00)00025-X)
- [14] Spindler, K., "Attitude Control of Underactuated Spacecraft", European Journal of Control, Vol. 6, Issue 3, 2000, pp. 229-242. [https://doi.org/10.1016/S0947-3580\(00\)71130-7](https://doi.org/10.1016/S0947-3580(00)71130-7)
- [15] Biggs, J.D., and Fournier, H., "Neural-network-based optimal attitude control using four impulsive thrusters", Journal of Guidance, Control, and Dynamics, 2020, pp. 299-309. <https://doi.org/10.2514/1.G004226>
- [16] Jin, L., and Xu, S., "Underactuated spacecraft angular velocity stabilization and three-axis attitude stabilization using two single gimbal control moment gyros", Acta Mechanica Sinica, Vol.26, Issue 2, 2010, pp. 279–288. <https://doi.org/10.1007/s10409-009-0272-4>
- [17] Gui, H., Vukovich, G., and Xu, S., "Attitude stabilization of a spacecraft with two parallel control moment gyroscopes", Journal of Guidance, Control, and Dynamics, Vol.39, No.3, 2016, pp. 728–735, <https://doi.org/10.2514/1.G000982>
- [18] Gui, H., Jin, L., Xu, S., and Zhang, J., "On the attitude stabilization of a rigid spacecraft using two skew control moment gyros", Nonlinear Dynamics, Vol.79, No.3, 2015, pp. 2079–2097. <https://doi.org/10.1007/s11071-014-1796-0>
- [19] Schaub, H., Junkins J. L., "Analytical Mechanics of Space Systems, Fourth Edition", AIAA Education Series, eISBN: 978-1-60086-155-0, 2018, pp. 179-186. <https://doi.org/10.2514/4.105210>
- [20] Yoon, H., and Tsotras, P., "Spacecraft Line-of-Sight Control Using a Single Variable-Speed Control Moment Gyro", Journal of guidance, control, and dynamics, Vol.29, No.6, 2006, pp. 1295-1308. <https://doi.org/10.2514/1.18777>
- [21] Sherrill, R.E., "Dynamics and Control of Satellite Relative Motion in Elliptic Orbits using Lyapunov-Floquet Theory", PhD Thesis, Auburn University, 2013, pp. 16-24. <http://hdl.handle.net/10415/3594>
- [22] Murray, R.M., Li, Z., and Sastry, S.S., "A Mathematical Introduction to Robotic Manipulation", Published by CRC Press, Taylor and Francis Group, 1994 pp. 179-188.
- [23] Mukherjee, R., and Chen, D., "Asymptotic Stability Theorem for Autonomous Systems", Journal of Guidance, Control, and Dynamics, 1993, pp. 961-963. <https://doi.org/10.2514/3.21108>
- [24] Romero-Calvo, A., Biggs, J.D., and Topputo, F., "Attitude Control For the LUMIO CubeSat in Deep Space", 70th International Astronautical Congress, IAC-19,C1,6,4,x50894, 2019, pp. 1-13. <http://hdl.handle.net/11311/1117585>